This is to certify that the
dissertation entitled

APPLICATION OF BORON-DOPED DIAMOND ELECTRODES FOR METAL ION ANALYSIS BY ANODIC STRIPPING VOLTAMMETRY

presented by

ELIZABETH ANN MCGAW

has been accepted towards fulfillment
of the requirements for the

Ph.D. degree in Chemistry

Greg M. Swain
Major Professor's Signature

May 18, 2007
Date

APPLICATION OF BORON-DOPED DIAMOND ELECTRODES FOR METAL ION ANALYSIS BY ANODIC STRIPPING VOLTAMMETRY

By

Elizabeth Ann McGaw

A DISSERTATION

Submitted to
Michigan State University
in partial fulfillment of the requirements
for the degree of

DOCTOR OF PHILOSOPHY

Department of Chemistry

2007

ABSTRACT

APPLICATION OF BORON-DOPED DIAMOND ELECTRODES FOR METAL ION ANALYSIS BY ANODIC STRIPPING VOLTAMMETRY

By

Elizabeth Ann McGaw

Anodic stripping voltammetry (ASV) is an established method for monitoring heavy metal ions, and the overall aim of this work was to fully evaluate and understand the properties of boron-doped diamond (BDD) as they relate to its use in ASV. In order to fully characterize the properties of BDD, several inquiries were conducted: (i) comparison of the electrochemical properties and response with the traditional Hg electrode, (ii) exploration of the utility of the material in microgravity, (iii) determination of the usefulness of BDD for more complex matrices (e.g., urine, blood), and (iv) investigation of ways of preventing electrode fouling (e.g., coatings, complexing agents) in solutions containing high protein concentrations (e.g., whole blood).

In addition to having many of the desirable features of Hg, BDD has some inherent advantages over Hg electrodes; it is non-volatile and non-toxic. BDD has a wider anodic potential limit and a lower background current density than Hg. Both BDD and Hg coated glassy carbon (Hg-GC) provided detection limits for all the metal ions (Zn^{2+}, Cd^{2+}, Pb^{2+}, Cu^{2+}, Ag^{+}) in the mid to low ppb range ($S/N \geq 3$). Although the magnitude of the stripping peak current and charge were greater for Hg-GC; this was offset by a comparable reduction in the background noise for BDD resulting comparable or lower limit of detection values.

The utility of BDD for ASV analysis of heavy metal ions (e.g., Ag^+) in the water supply on-board the International Space Station (ISS) was also investigated. A concentrated buffer solution allows adjustment of the solution conditions (e.g., pH, electrolyte concentration) and a prototype cell for microgravity was developed. Because elimination of the N_2 purge step was necessary for this application, dissolved O_2 was determined to have some effect on Pb^{2+} and Cu^{2+} determinations. The use of an oxygen scavenging molecule (ascorbic acid) to chemically remove the O_2 mitigated this problem to a large extent. BDD was found to exhibit good long-term response stability for Ag^+ (<10% relative standard deviation in response over 90 days). Analysis of simulated water samples in the microgravity cell using BDD yielded accurate Ag^+ concentrations (< 5% error).

BDD was also used for ASV analysis of metal ions in biological matrices. A linear calibration curve (10 – 250 ppb) was obtained in a urine simulant and the response was reproducible electrode-to-electrode (RSD 6%). Stability tests in a rat urine sample showed no fouling effects over a 6-hour period. Although BDD is resistant to fouling, it cannot be used directly in whole blood. However, Nafion-coated BDD is successfully used for Pb^{2+} analysis with a linear calibration response ($r^2 > 0.98$). A solution-based fouling prevention method using sodium dodecyl sulfate (SDS) to aggregate with the blood protein was also promising. When the electrolyte contained SDS, the signal for Pb^{2+} obtained in the presence of albumin was comparable to the signal obtained in a standard solution.

ACKNOWLEDGMENTS

There have been many people that have helped me during my time here at Michigan State. First, I would like to thank my advisor, Dr. Greg Swain, for giving me a place to learn and grow, and for all of the guidance and encouragement. I would also like to thank my committee members, Dr. Merlin Bruening, Dr. Gavin Reid, and Dr. Keith Lookingland. All of their input and support has been very valuable to me throughout this process.

To Dr. Kathy Severin and all of the fellow members of Women in Chemistry, so fondly known as WiC – thanks for all the fun we had and all of the things we accomplished. It was great to have an opportunity to participate in so many outreach opportunities, and a good excuse to get out of the lab once and awhile!

I need to thank all of my labmates, past (Prerna, Stotter, Grace, Jesse, Gloria, Anne, Bennett, Yang, Audrey, Luther, Veronika, Jason T, and Bhavik) and present (Wang, Hua, Yingrui, Matt Swope, Ayten, Isao, Martin, Dasa, Michael, Lisa, Matt Smith, and Jia) for all of their support. For all of you who have left before me I miss all of you and the guidance, discussions, and fun we had. For the current members I wish you the best of luck as you go on to pursue your dreams. The lab is a constantly changing environment as different people come and go and all of you have added special memories to my time in graduate school and I will not forget you.

And finally, I need to thank my friends and family for their encouragement. For Mel, you've been here with me since the beginning and it has been wonderful to share everything with such a great friend. To everyone else, Amber, Audrey, Luther, Anne, Carl and JB, thanks for listening when I had silly questions and for keeping me sane while I was trying to finish two degrees at once. I will miss all of the times we shared and hope that we can continue to stay in touch since we are now spread all over the country. To my parents for all of their love and support and for teaching me a strong work ethic that has gotten me through graduate school. To Scott, thank you for all of your love throughout all of this and being willing to tolerate me coming home late day after day, I could not have done this without you by my side.

TABLE OF CONTENTS

LIST OF TABLES

LIST OF FIGURES

CHAPTER 1

INTRODUCTION

1.1. Background

Monitoring heavy metal ion levels is essential for human health and safety. There are numerous health problems associated with exposure to high levels of metal ions (e.g., Cd^{2+}, Pb^{2+}, Hg^{2+}, $As^{3+/5+}$) because of their tendency to accumulate in the body and their low rate of clearance. For instance, the biological half-life of Cd is 10 to 30 years and the half-life of Pb in bone is more than 20 years.[1] There are many routes for contaminant exposure: water, food supply, air, and environment/occupation exposure (e.g., steel production). The Environmental Protection Agency (EPA) estimates that nearly twenty percent of human exposure to Pb is through contaminated drinking water.[2] It is, therefore, critical for humans to experience minimal exposure to these contaminants and this can be accomplished through effective water quality monitoring.

Regulatory agencies, such as the EPA, have established maximum allowable contaminant levels in drinking water to ensure public health. These standards are meaningless, though, unless analytical methods exist that can monitor these contaminants with adequate sensitivity, selectivity, and reproducibility. The present EPA recommended methods for metal ion analysis in water are atomic absorption spectroscopy (AAS), inductively couple plasma mass spectrometry (ICP-MS), and anodic stripping voltammetry (ASV). ASV is commonly employed because of its wide linear dynamic range, low detection limit (ppb), and multielement analysis capability. An additional advantage of ASV,

over AAS or ICP-MS, is the simplicity of the instrumentation, which is relatively inexpensive, small in size, requires low electrical power, and is portable enabling its field deployment.

In addition to environmental monitoring there is also need for analysis of clinical samples (e.g., blood, urine) that may contain heavy metals. Since the metals are toxic to humans the concentration of metal determined in these fluids can help diagnose clinical symptoms. In some cases, such as symptomatic patients with high levels of Pb^{2+}, chelation therapy can be effective.[1] Chelation therapy involves administering a chelating agent, with ethylenediamine tetraacetic acid (EDTA) being the most common. These agents complex the toxic metal ion and aid in its removal from the body. Analysis of the metal ions in body fluids can also be useful for monitoring the effectiveness of this treatment.

Currently, the most common method for analysis of metal ions in body fluids is AAS, typically using a graphite furnace to atomize the samples for detection.[3-6] The use of ASV for clinical samples also has some advantages, particularly the portability and low cost of the instrumentation that would make it practical for use in a doctor's office or at bedside. In fact, there is a commercially available Pb^{2+} analysis system marketed by BAS, Inc. (LeadCare) that is based on ASV.

1.2. Anodic Stripping Voltammetry

ASV is an electroanalytical technique in which the current at the working electrode is measured as a function of a potential waveform applied to the working electrode. The working electrode is the electrode at which the

electrochemical reaction of interest takes place. The applied potential controls the reducing or oxidizing strength of the electrode.

Stripping voltammetry gains advantages in sensitivity and detection limit because of an initial preconcentration step. The deposition potential is chosen to be more negative than the standard reduction potential (E^0) of the analyte in order to reduce and deposit the metal ion on the surface. The deposition can vary from seconds to minutes.

Once the analyte has been preconcentrated/deposited, it is then stripped off by applying a positive-going (anodic) potential. The current is recorded during this step, and can provide both qualitative and quantitative information. The oxidation of the metal will occur near the reversible Nernstain potential (E^0) for the metal, so the potential at which the highest current is obtained will serve to identify the metal present. The magnitude of this current can be used to plot calibration curves and to determine the metal ion concentration in the bulk solution. An example of the voltammetric *i-E* curve obtained for a solution containing two metal ions is shown in Figure 1.1; the dashed lines demonstrate the correlation of the potential waveform (top) and the voltammetric *i-E* curve (bottom).

There are several variations on the simple case of linear scan stripping voltammetry that change the way the positive potential sweep is carried out in order to reduce the contribution of the background charging current. In linear sweep voltammetry the total current is recorded and is a combination of background current and faradaic current. However, only the faradaic current

reflects the oxidation of the metal. The charging current is created by changing the potential across the electrode-solution interface, which acts as a capacitor. When a potential is applied to the working electrode the charge must be balanced on the solution side with an array of ions and oriented dipoles. This separation of charge at the electrode-solution interface creates a capacitor; potential changes create a current (charging current) that flows to charge and discharge this capacitor.

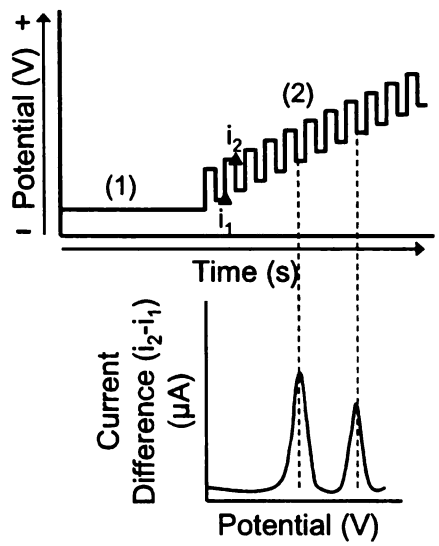

Figure 1.1. Differential pulse anodic stripping voltammetry (DPASV) waveform (top), and voltammetric *i-E* curve (bottom) for a solution containing two metals. The deposition step (1) followed by the stripping step (2). The current is sampled at two points noted by ▲, the current difference ($i_2 - i_1$) is plotted versus potential.

Differential pulse anodic stripping voltammetry (DPASV) is a common technique used to minimize the contribution of the charging current. The potential waveform is shown in Figure 1.1. In this technique, pulses of equal amplitude are superimposed upon the linear scan. The current is sampled at two points, one just before the pulse is applied and one just before the pulse is

finished, the former is subtracted from the latter and this difference is plotted versus the potential. This takes advantage of the different decay rates of faradaic and charging currents, since charging currents decay exponentially with time and faradaic currents only decay with $t^{-1/2}$. The pulse width is such that when the current is sampled it will be mostly faradaic. It is assumed that the charging current at both sampling points will be approximately the same so any differences can be attributed to faradaic current.

1.3. Working Electrodes

The choice of working electrode is critical for high quality ASV measurements. Many different factors can influence the performance of a working electrode. The first ASV studies were performed using Pt; however, it was quickly realized that Hg had superior properties. These properties include a large negative potential window, reproducible response, and good sensitivity.[7] Hg is used in several forms. Initially, an Hg-coated Pt electrode was used, which then evolved into the Hg pool electrode, and then to a hanging drop.[8-13] In 1970, Florence proposed co-deposition of Hg and the analyte metals onto a glassy carbon surface in the form of a thin film.[14] This thin layer Hg electrode exhibited increased peak resolution as compared to the hanging-drop or even thicker films of Hg. This is still one of the more commonly used Hg electrode preparation methods for ASV because it is simple and leads to reproducible results.

Hg is unique when compared to other electrodes because it forms an amalgam with the analyte metals. This reduces surface interactions and intermetallic compound formation, both of which can cause distortion in the shape

of the stripping voltammetric *i-E* curves. Even with these attributes, however, alternate electrodes are desired because of Hg's toxicity and volatility.

There are some specific interactions of electrodes with analytes that can enhance the signal. For example, an interaction between As^{3+} and Au makes it the best choice for analysis of As^{3+}.[15] The other consideration is the matrix components and the effect they may have on the working electrode. For instance, Cl^- interacts with a Hg surface forming calomel (HgCl) which will affect the electrochemical response. Therefore, Hg is not a good choice for use in a matrix containing Cl^-.

Several alternate electrodes to Hg have been investigated, such as Ir,[16, 17] Au,[18-22] Ag,[23, 24] and boron-doped diamond (BDD).[25-36] One alternative that has shown promising behavior for stripping analysis is Bi-modified electrodes, as studied by the Wang group[37-41] and others.[42] Bismuth can be co-deposited with the contaminant metals, similar to the preparation of a Hg-film electrode, and this electrode provides detection figures of merit that are comparable to those for Hg. A limiting factor with Bi, however, is the low anodic potential limit.

1.4. Diamond Electrodes

Diamond is also an attractive alternative with properties similar to those of Hg. The comparison of these properties is presented in Table 1.1. BDD has a wider potential window than Hg, and has been found to yield good detection figures of merit for many metal ions. One of the very first metal ions investigated with BDD using ASV was Pb^{2+}. Fujishima and co-workers demonstrated a low ppb limit of detection on a bare diamond using a preconcentration time of 15

min.[26] The more positive potential limit of BDD has been exploited in detection of Hg^{2+} with detection limits in the low ppb range for short preconcentration times (30 s), and in the mid-ppt range for longer deposition times (20 min).[29, 32] The Compton group has investigated the enhancing effects of ultrasound on the stripping current, and showed detection limits with BDD in the high ppt range for Ag^{+} and Cd^{2+}.[27, 34] The stripping current can also be enhanced with microwaves focused in the vicinity of the BDD surface. This lowered the detection limit for Pb^{2+} by an order of magnitude, likely due to enhanced convective mass transport from the temperature gradients created.[28]

Table 1.1. Comparison of the electrochemical properties of BDD and Hg electrodes for use in anodic stripping voltammetry.

Boron Doped Diamond (BDD)	**Hg**
Wide cathodic and anodic potential limits	Wide cathodic limit
Lower background current	Higher background current
Good sensitivity	Good sensitivity
Chemically inert	Interaction with Cl^{-}
Reusable surface – no pretreatment required	Easily refreshed surface
Non-toxic	Toxic
Non-volatile	Volatile

Early work from our group showed the usefulness of BDD for real sample analysis, such as river, and tap waters, as well as digests of waste treatment sludge, and soils.[31] The accuracy of the method using this electrode was demonstrated using a standard reference material (SRM) obtained from the National Institute for Standards and Technology (NIST). The anodic stripping voltammetric *i-E* curve recorded for the SRM sample is shown in Figure 1.2. Comparison curves for solutions (acetate buffer, pH 4.5) containing Pb^{2+}, Cu^{2+},

and Ag^+ in equal concentrations ranging from 10 – 90 ppb are also shown. The metal ion concentrations in the SRM were determined using the standard addition method and the resulting values are shown in Table 1.2. The solution was also analyzed by flame atomic absorption spectroscopy (AAS), and the results are also shown in the table.

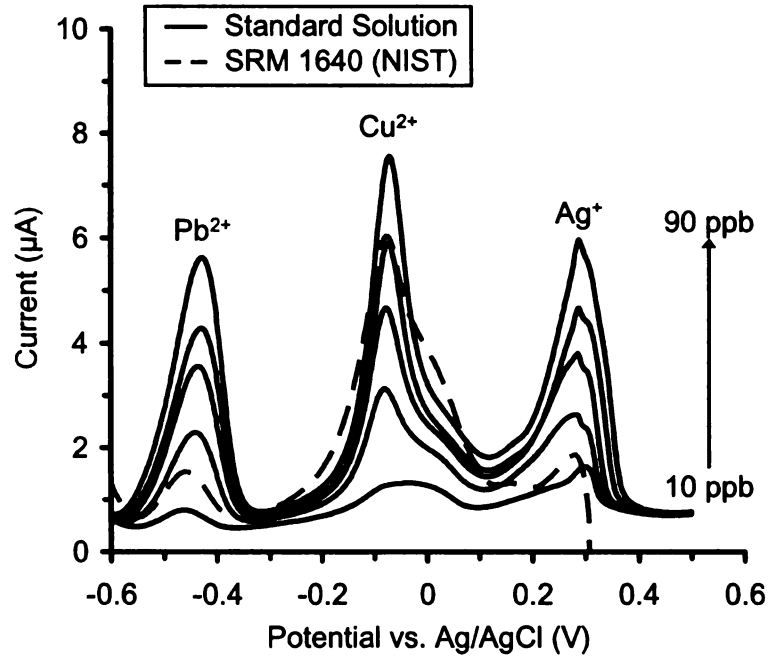

Figure 1.2. Anodic stripping voltammetric *i-E* curves for a standard reference solution obtained from NIST (SRM - NIST 1640). Voltammetric curves for standard solutions, in acetate buffer, pH 4.5, of equal concentrations of containing Pb^{2+}, Cu^{2+}, and Ag^+ are also shown. Deposition was for 180 s at -0.9 V vs. Ag/AgCl. Figure reproduced with permission from Elsevier.[31]

The values determine by ASV compare favorably to both the NIST certified values (error ≤ 10%) as well as to AAS values, the latter is a well established technique for metal ion analysis. This result demonstrates the capability of multimetal ion analysis with BDD using ASV.

Table 1.2. Analysis of NIST SRM 1640. Comparison of concentrations determined by anodic stripping voltammetry (ASV) and atomic absorption spectroscopy (AAS). The error reported for each analytical method is compared to NIST certified values.[31]

	Pb^{2+} NIST: 27.89 ± 0.14		Cu^{2+} NIST: 85.2 ± 1.2		Ag^{+} NIST: 7.62 ± 0.25	
	Concentration (ppb)	Error	Concentration (ppb)	Error	Concentration (ppb)	Error
ASV	30.2 ± 0.8	8%	77 ± 3	10%	7.3 ± 0.6	4%
AAS	25 ± 2	10%	89.3 ± 0.6	5%	8.0 ± 0.7	5%

In addition to the aqueous samples some additional solid samples were tested: soil and sludge. The sludge was obtained from a wastewater treatment facility, and heavy metals and other unwanted materials (e.g., organic components not easily biodegradable) collect in this material. In order to analyze the sludge, and similarly the soil, an acid digestion (concentrated HNO_3) was used to solubilize the metals. Two metals were detected in the sludge, Cd and Pb, and were quantified using standard addition. The stripping voltammetric *i-E* curve obtained for the sludge digest is displayed in Figure 1.3 and is compared to standard solutions of Cd^{2+} and Pb^{2+}.

Concentrations of metal in the acid digest of the sludge sample were determined by AAS well, and the results obtained by ASV are compared to the AAS results in Table 1.3. Again the results from ASV on BDD compare favorably with the established technique, AAS.

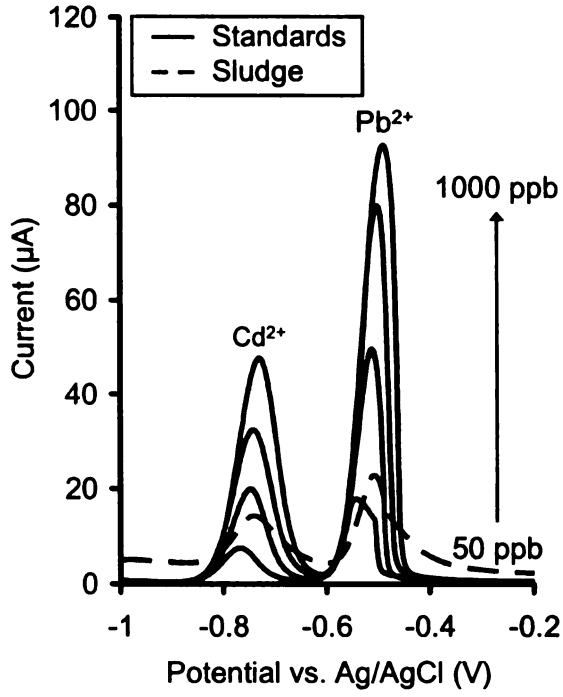

Figure 1.3. Anodic stripping voltammetric *i-E* curve for sludge, overlaid with responses for standard solutions, in acetate buffer, pH 4.5, containing Cd^{2+} and Pb^{2+} in equal concentrations ranging from 50 to 1000 ppb. The deposition time was 180 s at -1.0 V vs. Ag/AgCl. Image reprinted with permission from Elsevier.[31]

Table 1.3. Concentrations of Cd^{2+} and Pb^{2+} in the acid digest of the waste treatment sludge as determined by ASV and AAS.[31] The error is the difference between the two techniques.

	ASV (ppb)	AAS (ppb)	Error
Cd^{2+}	156 ± 5	145 ± 3	7.5%
Pb^{2+}	124 ± 5	134 ± 2	8.1%

Other groups have also verified results from ASV analysis on BDD with more traditional techniques (e.g., ICP-AES, AAS) with favorable results.[28, 33] For example, Babyak and Smart compared concentrations of Cd^{2+} determined for a sample of spiked river water using ASV on BDD and ICP-AES (atomic emission

spectroscopy) and found there was an error of 8.7% between the two techniques (59.8 ppb and 55 ppb determined with ASV and ICP-AES, respectively).[33] Overall BDD has been successfully used for ASV analysis and is a potential alternative to the Hg-based electrodes.

1.5. Dissertation Overview

Earlier work has shown that BDD is a suitable electrode for analysis of a variety of samples including natural waters, soils, and sludge using ASV. The focus of this project was to further explore the properties of BDD for ASV. While BDD has been shown to be useful for ASV analysis there has not been any direct comparison of the BDD and the Hg-based electrodes traditionally used. This study serves to investigate the properties of BDD including analytical figures of merit, manner of metal deposition, stripping peak potentials, and shapes as compared to a Hg-coated glassy carbon electrode. BDD has advantages over Hg, particularly the non-toxic, non-volatile nature of the electrode. Since BDD has already been used for ASV analysis the goal was to determine the similarities and differences in the electrode performance with respect to Hg and the utility as an alternate electrode.

One particular application of BDD that was of interest was to develop a method for heavy metal analysis in microgravity. On-board the International Space Station (ISS) Ag^+ is used as a biocide in the water supply, and a method was needed to analyze the metal ion content (both Ag^+ as well as potential contaminants) continuously or semi-continuously to maintain a safe water supply.[36, 43-45] ASV was the method chosen for analysis because of its portability

and low power requirements, but because of the toxicity and volatility of Hg the use of a Hg electrode in microgravity is not possible. The properties of BDD (e.g., non-toxic, non-volatile) and the comparable electrochemical response to Hg electrodes make BDD a good alternate electrode for this application. In developing a method for on-board use several issues had to be addressed including addition of electrolyte, constraints of microgravity, and long-term stability of the method. Because the water samples of interest were potable and technical (used for toilet flushing, hygiene, etc.) waters, they contained minimal amounts of electrolyte and the pH could vary. There were also many challenges encountered to modify the method for microgravity: all of the liquid had to be enclosed, the pH needed to be between 5.5 and 9, and deoxygenation using N_2 sparging was not possible. Addressing the needs of an assay in microgravity and determining the performance of the BDD electrode was the main focus of this portion of the work.

BDD has been successfully applied to environmental and water samples. The hydrophobic nature of the electrode surface tends to make this electrode fouling resistant which could be very beneficial to use in a more complex matrix than a water sample or a soil digest sample. Biological samples (e.g., blood, urine) are particularly troublesome for electrochemical methods because of the number of components (e.g., proteins, biomolecules) that can foul the electrode surface; therefore, these samples were chosen to probe the fouling resistance of BDD.

A simulated urine sample was used initially to explore the stability and anti-fouling nature of the BDD surface. In urine samples, the concentration of metal ions is low (high ppt to low ppb), and therefore, the deposition conditions were optimized in order to obtain the lowest detection limits. The analytical figures of merit were measured to gauge the performance of the BDD electrode. A sample of rat urine was also tested on the BDD surface and a series of measurements were made over the course of several hours in order to determine the stability of the BDD response in the urine matrix.

Blood was the other biological fluid that was tested on the BDD electrodes. Blood is a much more complex matrix than urine, containing a much higher concentration of proteins as compared to urine. In metal analysis the blood needs to be analyzed whole (i.e., not plasma) because the metal ions are bound to the red blood cells. Even though BDD has a fouling resistant surface it is still not able to be used directly in a blood solution. Therefore, two options were explored to protect the electrode from fouling. A polymer coating (Nafion) was used to physically block the proteins from reaching the electrode surface, and a solution based complexing agent (sodium dodecyl sulfate) for the proteins was used to prevent fouling. The effectiveness of each of these methods was explored.

The aims of this project were to further explore the properties of BDD for ASV analysis, specifically to: (i) compare the electrochemical properties and response to a traditional Hg electrode, (ii) explore the utility in microgravity applications, (iii) determine the usefulness of BDD for more complex matrices

(e.g., urine, blood), and (iv) to explore potential fouling prevention methods (e.g., coatings, complexing agents) to use BDD in solutions containing high protein concentrations (e.g., whole blood).

1.6. References

(1) Goyer, R. A. In *Casarett & Doull's Toxicology: The Basic Science of Poisons,* 5th ed.; Klaassen, C. D., Ed.; McGraw-Hill: New York, 1996, pp 691-736.

(2) Drinking Water Standards. http://www.epa.gov/safewater/standards.html (accessed May 2007)

(3) Sharma, R. P.; McKenzie, J. M.; T., K. *J. Anal. Tox.* **1982**, *6*, 135-138.

(4) Plotkin, E.; McAleer, J. F.; Cordeiro, M. L.; Ackland, M. R.; Sheehan, T. M.; Braithwaite, R. A. *Clin. Chem.* **1997**, *43*, 2187-2189.

(5) Yassin, A. S.; Martonik, J. F. *J. Occup. Environ. Hyg.* **2004**, *1*, 324-333.

(6) Castro Maciel, C. J.; Miranda, G. M.; Oliveria, D. P.; Siqueria, M. E. P. B.; Silveria, J. N.; Leite, E. M. A.; Silva, J. B. B. *Anal. Chim. Acta* **2003**, *491*, 231-237.

(7) Lord, S. S.; O'Neill, R. C.; Rogers, L. B. *Anal. Chem.* **1952**, *24*, 209-213.

(8) Gardiner, K. W.; Rogers, L. B. *Anal. Chem.* **1953**, *25*, 1393-1397.

(9) Porter II, J. T.; Cooke, W. D. *J. Am. Chem. Soc.* **1955**, *77*, 1481-1486.

(10) Ross, J. W.; DeMars, R. D.; Shain, I. *Anal. Chem.* **1956**, *28*, 1768-1771.

(11) Mamantov, G.; Papoff, P.; Delahay, P. *J. Am. Chem. Soc.* **1957**, *79*, 4034-4040.

(12) Nikelly, J. G.; Cooke, W. D. *Anal. Chem.* **1957**, *29*, 933-939.

(13) DeMars, R. D.; Shain, I. *Anal. Chem.* **1957**, *29*, 1825-1827.

(14) Florence, T. M. *J. Electroanal. Chem. Interfacial Electrochem.* **1970**, *27*, 272-281.

(15) Song, Y.; Swain, G. M. *Anal. Chem.* **2007**, *79*, 2412-2420.

(16) Nolan, M. A. *Anal. Chem.* **1999**, *71*, 3567-3573.

(17) Herdan, J.; Feeney, R.; Kounaves, S. P.; Flannery, A. F.; Storment, C. W.; Kovacs, G. T. A.; Darling, R. B. *Environ. Sci. Technol.* **1998**, *32*, 131-136.

(18) Andrews, R. W.; Johnson, D. C. *Anal. Chem.* **1975**, *47*, 294-299.

(19) Wang, J.; Tian, B. *Anal. Chem.* **1993**, *65*, 1529-1532.

(20) Viltchinskaia, E. A.; Zeigman, L. L.; Morton, S. G. *Electroanal.* **1995**, *7*, 264-269.

(21) Bonfil, Y.; Brand, M.; Kirowa-Eisner, E. *Anal. Chim. Acta* **1999**, *387*, 85-95.

(22) Feeney, R.; Kounaves, S. P. *Anal. Chem.* **2000**, *72*, 2222-2228.

(23) Kirowa-Eisner, E.; Brand, M.; Tzur, D. *Anal. Chim. Acta* **1999**, *385*, 325-335.

(24) Bonfil, Y.; Kirowa-Eisner, E. *Anal. Chim. Acta* **2002**, *457*, 285-296.

(25) Saterlay, A. J.; Foord, J. S.; Compton, R. G. *Analyst* **1999**, *124*, 1791-1796.

(26) Manivannan, A.; Tyrk, D. A.; Fujishima, A. *Electrochem. Solid-State Lett.* **1999**, *2*, 455-456.

(27) Saterlay, A. J.; Marken, F.; Foord, J. S.; Compton, R. G. *Talanta* **2000**, *53*, 403-415.

(28) Tsai, Y.-C.; Coles, B. A.; Holt, K.; Foord, J. S.; Marken, F.; Compton, R. G. *Electroanal.* **2001**, *13*, 831-835.

(29) Manivannan, A.; Seehera, M. S.; Tryk, D. A.; Fujishima, A. *Anal. Lett.* **2002**, *35*, 355-368.

(30) Show, Y.; Witek, M. A.; Sonthalia, P.; Swain, G. M. *Chem. Mater.* **2003**, *15*, 879.

(31) Sonthalia, P.; McGaw, E.; Swain, G. M. *Anal. Chim. Acta* **2004**, *522*, 35-44.

(32) Manivannan, A.; Seehra, M. S.; Fujishima, A. *Fuel Process. Technol.* **2004**, *85*, 513-519.

(33) Babyak, C.; Smart, R. B. *Electroanal.* **2004**, *16*, 175-182.

(34) Banks, C. E.; Hyde, M. E.; Tomcik, P.; Jacobs, R.; Compton, R. G. *Talanta* **2004**, *62*, 279-286.

(35) Wantz, F.; Banks, C. E.; Compton, R. G. *Electroanal.* **2005**, *17*, 655-661.

(36) McGaw, E.; Sonthalia, P.; Swain, G. M. *SAE Technical Paper 2005-01-2888 35th International Conference on Environmental Systems* **2005**.

(37) Wang, J.; Lu, J.; Hocevar, S. B.; Farias, P. A. M.; Ogorevc, B. *Anal. Chem.* **2000**, *72*, 3218-3222.

(38) Wang, J.; Lu, J.; Hocevar, S. B.; Ogorevc, B. *Electroanal.* **2001**, *13*, 13-16.

(39) Wang, J.; Lu, J.; Kirgoz, U. A.; Hocevar, S. B.; Ogorevc, B. *Anal. Chim. Acta* **2001**, *434*, 29-34.

(40) Flechsig, G.-U.; Korbout, O.; Hocevar, S. B.; Thongngamdee, S.; Ogorevc, B.; Grundler, P.; Wang, J. *Electroanal.* **2002**, *14*, 192-196.

(41) Pauliukaite, R.; Hocevar, S. B.; Ogorevc, B.; Wang, J. *Electroanal.* **2004**, *16*, 719-723.

(42) Kruusma, J.; Banks, C. E.; Compton, R. G. *Anal. Bioanal. Chem.* **2004**, *379*, 700-706.

(43) Plumlee, D. K.; Mudgett, P. D.; Schultz, J. R. *SAE Technical Paper 2002-01-2537 32nd International Conference on Environmental Systems* **2002**.

(44) Mudgett, P. D.; Benoit, M. J.; Schultz, J. R. *SAE Technical Paper 2002-01-2532 32nd International Conference on Environmental Systems* **2002**.

(45) Plumlee, D. K.; Mudgett, P. D.; Schultz, J. R. *SAE Technical Paper 2003-01-2401 33rd International Conference on Environmental Systems* **2003**.

CHAPTER 2

EXPERIMENTAL METHODS

2.1. Diamond Thin Film Deposition

Nanocrystalline diamond thin-film electrodes were used in all of the studies detailed in this work. The nanocrystalline diamond was deposited on highly conductive p-type Si (~10^{-3} Ω-cm) (Virginia Semiconductor, Inc.) by microwave-assisted chemical vapor deposition (CVD) (1.5 kW, 2.54 GHz, Model AX3120, Astex, Inc., Lowell, MA).[1] A schematic of this reactor is shown in Figure 2.1. The Si substrate was first prepared by scratching the surface with a 0-2 μm diameter diamond powder (GE Superabrasives, Worthington, OH) in an ultrapure water slurry. After scratching the substrates were rinsed with ultrapure water and isopropanol. The surface was further cleaned by sonication (5 min each) in acetone, isopropanol, and water, sequentially. The clean substrates were dried and examined under a polarized light microscope (Olympus BX60M, Olympus America, Inc.) to check for surface cleanliness. If polishing debris remained on the surface the substrates were resonicated until it was removed. The preparation by scratching the surface was necessary to create defects in the Si surface and embed small diamond particles to serve as nucleation sites for diamond growth. It was important that a uniform density of scratches was present on the surface to obtain uniform diamond film growth.

Once the substrates were clean they were placed on a sample stage made up of layers starting with a stainless steel plate, Mo, W, quartz, and finally the Si substrate. The sample stage was loaded into the reactor chamber,

consisting of a quartz bell jar that could be evacuated of atmospheric gases using a rotary pump. The chamber was allowed to pump down for at least 2 hours and a pressure of < 20 Torr was obtained. Following evacuation of atmospheric gasses the source gases were introduced into the chamber.

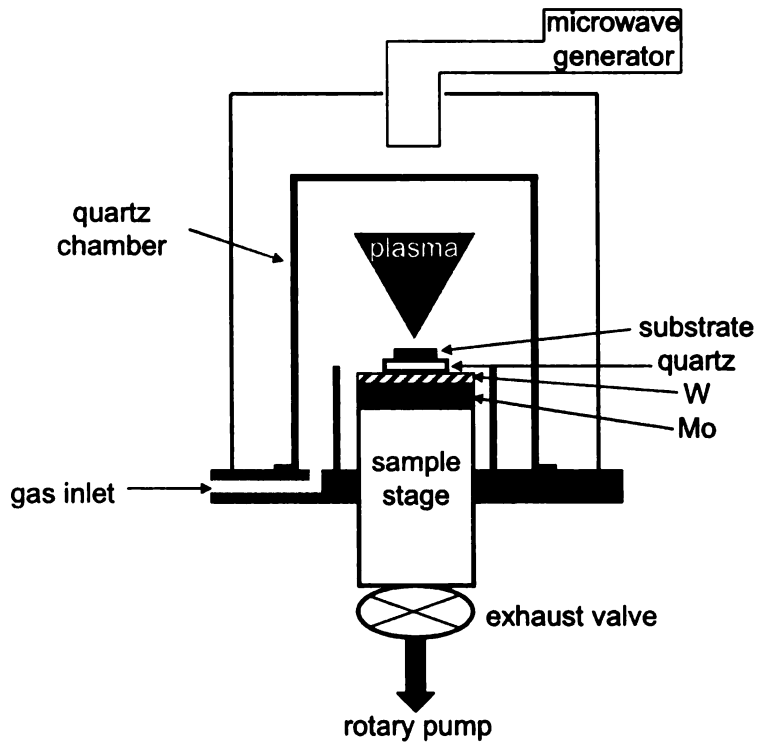

Figure 2.1. Schematic of microwave assisted chemical vapor deposition reactor used for diamond electrode growth.

The source gas mixture, containing ultrahigh-purity methane, hydrogen, and argon, entered the reactor at flow rates of 1, 5, and 94 sccm, respectively. All gases were ultrahigh purity (99.999%) grade (methane and hydrogen from AGA Specialty Gas, Cleveland, OH; argon from BOC Group, Inc., Murray Hill, NJ). Deposition was accomplished using a power of 800 W, a system pressure of 140 Torr, a substrate temperature estimated (optical pyrometry) to be between

700 and 800 ℃, and a deposition time of 2 h. Each film was boron-doped during deposition by adding 10 ppm diborane (0.1% B_2H_6 diluted in H_2) to the source gas mixture. At the end of the growth period, the film remained exposed to argon-hydrogen plasma for 10 min followed by a gradual reduction in power and pressure to slowly cool the film in the presence of atomic hydrogen. Post-growth annealing in atomic hydrogen is essential for removal of any adventitious non-diamond carbon and assurance of full hydrogen termination. After deposition, the film was cleaned by chemical oxidation, exposing the film to warm aqua-regia then to warm hydrogen peroxide (30%), each for 30 min. The film was then rehydrogenated in a hydrogen plasma (200 sccm H_2, 35 Torr, 1000 W) for 30 min, and cooled in the same manner as described for the growth procedure.[2] The resulting film thickness was approximately 5 μm, as determined by cross sectional scanning electron microscopy imaging. Hall effect measurements of other films grown in a similar manner revealed a carrier concentration (holes) in the low 10^{20} cm^{-3} range and a carrier mobility of 0.1 to 1 cm^2/V-s. The relatively low mobility (single crystal diamond ~3000 cm^2/V-s) results from electron scattering by the high fraction of grain boundary.

2.2. Material Characterization

2.2.1. Electrochemical Characterization

A single-compartment glass cell (~5 mL volume), shown in Figure 2.2, was used for the electrochemical measurements along with a computer-controlled potentiostat (Model 650B, 850, or 900 CH Instruments Inc., Austin, TX).[2] The electrochemical cell was housed inside a grounded Faraday cage for electrical

shielding. The working electrode was clamped against a Viton o-ring at the bottom of the cell to confine the solution. Prior to use, a small amount of carbon from a graphite rod was rubbed on the backside of the scratched and cleaned Si substrate to ensure good ohmic contact with the copper current-collector plate. The geometric area of the electrode exposed to the solution was 0.2 cm^2, unless otherwise noted. A large area carbon rod served as the counter electrode, and was placed normal to the working electrode. A Ag/AgCl reference electrode (saturated KCl, E^0 = -45 mV vs. SCE) was placed inside a cracked-glass capillary (double junction) and filled with the supporting electrolyte.

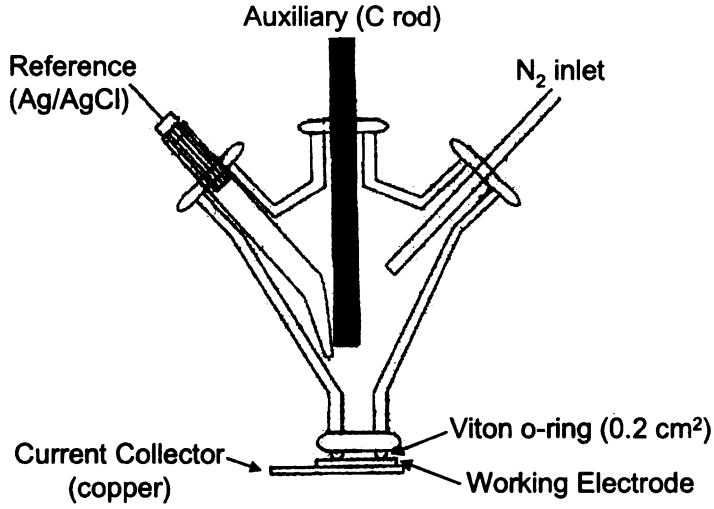

Figure 2.2. Diagram of electrochemical cell.

Prior to their use for stripping voltammetry experiments initial characterization experiments were performed on all new diamond electrodes to ensure they had similar electrochemical properties. Background cyclic voltammograms were measured in 0.1 M perchloric acid solution. The potential

was swept between approximately -1.5 V and 1.5 V vs. Ag/AgCl to determine the potential window. The potential window was defined as the region between ± 50 μA. The electrodes used had potential windows that spanned approximately 3 V. Cyclic voltammograms were also measured in 0.1 M ferrocyanide and 0.1 M ruthenium hexamine each in 1 M potassium chloride. The peak splitting was measured for scans taken at a 100 mV/s scan rate. The ferrocyanide is used to probe the surface cleanliness; a clean surface has a peak splitting close to 59 mV. Both the ferrocyanide and ruthenium hexamine probe the conductivity of the electrode, and a peak splitting of 59 mV indicates good conductivity. The diamond electrodes used had a peak splitting of approximately 70 mV for both analytes.

2.2.2. Raman Spectroscopy

Raman spectroscopy was used to study the microstructure of the diamond film. Spectra were obtained at room temperature using a Chromex RAMAN 2000 spectrograph (Chromex, Inc., Albuquerque, NM). The instrument consisted of a diode-pumped, frequency-doubled continuous wave Nd:YAG (yttrium aluminum garnet) laser (500 mW at 532 nm, COHERENT), a Chromex 500is spectrometer (f/4, 600 grooves/mm holographic grating, 50 μm slit width), and a charge-coupled device (CCD) detector (ANDOR Tech., Ltd.), 1024 x 256 element, thermoelectrically cooled. Spectra were collected with an incident power density of ~500 kW/cm^2, a 10 s integration time, and an approximate spectral resolution of 4 cm^{-1}. A white-light spectrum was collected and used as the background for

spectral correction. The Raman shift was calibrated using a spectrum of acetaminophen.

2.2.3. Resistivity Measurements

Resistivity of the diamond film is measured using a tungsten four point probe connected to an HP 3748A multimeter (Hewlett-Packard, Palo Alto, CA). The films used in this study showed semi metallic behavior and had resistivity values of < 0.05 Ω-cm.

2.3. Differential Pulse Anodic Stripping Voltammetry

Differential pulse anodic stripping voltammetry (DPASV) was used for metal analysis. The measurement involves two steps, first, a negative potential is applied for a fixed period of time to reduce the metal ions and form metal deposits on the electrode surface (i.e., preconcentration). Second, the potential is subsequently scanned toward positive values to selectively oxidize or "strip" the individual metals. In the present work, metal deposition was performed for 180 - 210 s (as noted in each chapter) at a potential sufficiently negative of the standard reduction potential. The deposition potentials for each metal ion were -1.3 , -1.0, -0.8, -0.4, and 0 V for Zn^{2+}, Cd^{2+}, Pb^{2+}, Cu^{2+}, and Ag^{+}, respectively. Differential pulse voltammetry was used for the positive (anodic) scan with the following parameters: a pulse height of 50 mV, a step height of 2 mV, a pulse width of 50 ms, and a cycle period of 100 ms. A constant potential of 0.600 V was applied for 180 s after completion of an anodic sweep to ensure full oxidation of all metal deposits. All measurements were made in an unstirred solution and at room temperature (~ 22-25 ℃).

2.4. Comparison to Hg Electrode

2.4.1. Hg-coated Electrode

The Hg-coated electrode was formed by electrodepositing the metal on glassy carbon (Hg-GC). Prior to use, the glassy carbon (GC-20 Tokai, Ltd.) was polished under clean conditions using a series of alumina slurries (1.0, 0.3, and 0.05 μm) (Buehler, Lake Bluff, IL) in water. The polishing debris was removed by ultrasonic cleaning for 15 min in ultrapure water after each polishing step. Finally, the polished electrode was soaked in distilled isopropanol for 15 min prior to use.[3] In a measurement, the Hg was co-deposited along with metal analyte from a 20 mM Hg^{2+} solution containing some concentration of the metal ion of interest.[4] The deposition potential used depended on the $E^{0'}$ for the M^{n+}/M redox couple but was sufficiently negative to co-deposit both Hg and the analyte metal.

2.4.2. Electrochemical Measurements

A 0.1 M acetate buffer, pH 5.2, with additional Ca^{2+} (30 ppm) and Mg^{2+} (5 ppm) ions served as the supporting electrolyte. Ca^{2+} and Mg^{2+} acetate salts were added to meet NASA requirements for potable water on-board ISS. It was determined that their presence did not affect the DPASV signal for any of the metal ion contaminants.[5] A cracked glass capillary was used to house the reference electrode (Ag/AgCl) to provide a barrier against Cl^- ion transport into the analyte solution; such leakage would cause complications with the measurement due to calomel formation. All solutions were purged with N_2 for at least 3 min prior to analysis in order to remove dissolved O_2. All measurements were made in an unstirred solution at room temperature (~22-25 ℃). Analysis

for the dissolved metal ions was carried out using DPASV as described previously with a deposition time of 210 s.

2.5. Microgravity Modification Experiments

2.5.1. Electrochemical Measurements

A glass cell would be unsafe for on-orbit use, so a specially-designed Teflon cell was used in this work. In the Teflon cell the working electrode was mounted from the bottom using the same size Viton o-rings as the glass cell described previously to define the working electrode area (~0.2 cm^2). Long-term potential stability of the reference electrode is an important consideration for on-board use of an electrochemical method. To this end, a "no-leak" Ag/AgCl reference electrode (EE-009, Cypress Systems, Inc., Lawrence, KS) has been incorporated which has similar stability to a standard Ag/AgCl reference electrode.

2.5.2. X-ray Diffraction Spectroscopy

Powder X-ray diffraction spectroscopy (XRD) was used to investigate the presences of metal deposits on the electrode surface following stripping. A Rikagu Rotaflex RTP300 RC (Tokyo, Japan) instrument was used. The anode used to generate the X-rays was a rotating Cu plate and the K1α X-ray line was used (1.540 Å). The scans were performed in the 2θ/θ mode at a scan rate of 1 degree/second.

2.4.3. Potable and Technical Water Simulants

Simulated Shuttle transfer water, potable (25-0203-02) and technical (25-0203-03) types, were provided by the Wyle Laboratory (Johnson Space Center).

Each of these waters contained Ag^+ in a concentration between 300 and 500 ppb. The potable water also contained Ca^{2+} and Mg^{2+} at concentrations of 30 ppm and 5 ppm, respectively. The analysis results for the Ag^+ concentrations determined by the Wyle laboratory using inductively-coupled plasma mass spectrometry (ICP-MS) were provided for each sample.

2.4.4. Microgravity Cell

A completely sealed electrochemical cell was designed for use in microgravity to fit the requirements that all liquids be contained. A diagram of this cell can be seen in Chapter 4, Figure 4.4. The body of the cell is made from Teflon, and the top is sealed with a polymethylmethacrylate (Plexiglas) so the inside of the cell could be visualized. There are 3 inlet and outlets on 3 of the sides that are fitted with luer fittings and valves to be compatible with the luer fittings on the current sampling bags used by NASA. The inner chamber is cubic with side length 18 mm, and a volume of 5-6 mL.

There is a swagelok fitting on the top of the Plexiglas cover that is intended for a Ag/AgCl "no-leak" electrode (EE-009, Cypress Systems, Inc., Lawrence, KS). The counter electrode consisted of a coiled Pt wire inserted through a small hole in the Teflon body, and sealed with silicon sealant (DAP, Inc., Baltimore, MD). The working electrode was a planar diamond thin-film that was sealed by a Viton o-ring (i.d. 1/4 inch, o.d. 5/16 inch) and had an exposed area of 0.32 cm^2, slightly larger than the conventional electrochemical cell.

The microgravity cell was used in conjunction with a portable potentiostat, PG580 (Princeton Applied Research, Oak Ridge, TN). This particular model is

about the size of a calculator, and can be used in a standalone mode or with a laptop computer. It can also be run on internal rechargeable batteries. In these studies the PG580 was run on battery power but was connected to a laptop computer for data acquisition.

2.6. Urine Analysis

2.6.1. Electrochemical Measurements

No additional supporting electrolyte was added to urine simulant and urine samples. For control samples 0.1 M acetate, pH adjusted to 8.8 (to match urine simulant) with sodium hydroxide, was used as the supporting electrolyte. All solutions were used within 1 week of preparation and stored in a refrigerator to prevent bacterial growth in the medium.

Before analysis, each solution was deoxygenated in the electrochemical cell by N_2 purging for at least 3 min. The N_2 purge was continued through the deposition and stripping steps as a source of convection. A flow meter was used to regulate the flow of N_2 day-to-day. A negative potential of -1 V was applied for 300 s (unless otherwise noted) to deposit Cd on the electrode surface. Following deposition, the metal was subsequently oxidized using DPASV as described previously. Following analysis, a cleaning step was performed by holding a positive potential ($\geq$ 0 V) for 180 s while purging with N_2 purge, to ensure that any Cd remaining on the surface is oxidized leaving a fresh BDD surface.

2.6.2. Simulated Urine and Rat Urine Samples

The components and concentrations used for the urine simulant were obtained from a NASA recipe for simulated early planetary base mission

wastewater.[6] The components are listed in Table 2.1 in order from highest to lowest concentration.

Table 2.1. Components and concentrations in simulated urine.

Component	Concentration
Ammonium Bicarbonate	250
Ammonium Hydroxide	100
Sodium Chloride	100
Potassium Bicarbonate	30
Creatinine	20
Potassium Dihydrogen	10
Hippuric Acid	7
Potassium Bisulfate	6
Lactic Acid	4
Citric Acid	3
DL-Tyrosine	3
D-Glucuronic Acid	2

After the components were mixed, the solution was sonicated for at least 15 minutes to ensure homogeneity.

Rat urine samples were obtained from the Galligan group from the Department of Pharmacology & Toxicology at Michigan State University. Several samples (2-3 mL) were obtained frozen (-20℃) in plastic vials. A larger volume was desired to allow for replicate measurements, therefore, 5 smaller samples (2-3 mL) were combined to generate a single homogenous sample that was approximately 10 mL. The combined sample was then centrifuged for 15 min, and the supernatant filtered with a syringe filter (PTFE, 0.1 μm). The sample was stored frozen (-20℃) until use.

2.7. Blood Analysis

2.7.1. Electrochemical Measurements

The analyte of interest for this study was Pb^{2+}. The Pb^{2+} is associated with the red blood cells, and digestion was necessary to release the Pb^{2+} for electrochemical analysis. Hydrochloric acid (0.3 M) was used and was mixed with the blood in a 5:1 (acid:blood) ratio. The sample was mixed directly in the electrochemical cell, first adding the acid followed by the blood. A Teflon cell, described above in the microgravity work, was used for the analysis of the blood samples. Glass is typically not used as it can cause the blood to coagulate.

2.7.2. Blood Sample

The blood obtained was bovine blood spiked with 47.2 µg/dL (~445 ppb) of Pb^{2+} and was stabilized with EDTA to prevent coagulation. The blood had also undergone two freeze/thaw cycles to lyse the red blood cells. These blood samples were obtained from ESA, Inc., and the Pb^{2+} was added by the scientists at ESA using the following procedure. The blood (Lampire Biological Laboratories, Pipersville, PA) was weighed and corrected for density (1.05 g/mL), then spiked with Pb^{2+} from a Pb^{2+} in DI water solution. The solution is rocked gently at room temperature for 4 hours to allow the blood to uptake the added Pb. Once the Pb^{2+} is added and allowed to mix the blood is analyzed by graphite furnace atomic absorption spectroscopy and/or isotope diluted mass spectrometry to confirm the concentration of Pb in the sample. The blood is then divided into small plastic vials (~2 mL) and is frozen for long term storage or

refrigerated for short term storage. Blood samples can be used for to 2-5 years if stored frozen.

2.7.3. Nafion Coating

A 3% Nafion solution was used to coat the diamond electrodes. The 3% solution was made by diluting a commercial 5% Nafion in ethanol solution (ElectroChem, Inc., Woburn, MA). 60 µL of the 3% solution was placed on the diamond film (~1 cm^2) using an Eppendorf pipet (Eppendorf, Hamburg). A single drop was placed in each corner of the square electrode and finally the center so the solution would be evenly distributed over the electrode surface. The electrodes were then allowed to air-dry on a flat surface. The electrodes were covered by a beaker during the drying process to prevent dust particles from settling into the polymer.

2.7.4. Atomic Force Microscopy

Atomic force microscopy (AFM) images were taken to determine if the Nafion coating was completely removed from the diamond surface using different cleaning methods. A Nanoscope III instrument (Veeco Metrology Group, Inc., Santa Barbara, CA) was used in the contact mode. Pyramidal-shaped Si_3N_4 tips, mounted on gold cantilevers (100 mm legs, 0.38 N/m spring constant), were used in air to acquire the topographical images. The scan rate ranged from 4 – 12 Hz depending on the scan size (0.5 – 3 µm).

2.8. Chemicals

All solutions were prepared with ultrapure water from an E-pure water purification system (Barnstead) having a resistivity greater than 17 MΩ-cm.

Cadmium nitrate, 99.999% (Sigma-Aldrich), zinc acetate, 99.999% (Sigma-Aldrich), cupric nitrate, 99.999% (Sigma-Aldrich), lead nitrate, 99.999% (Sigma-Aldrich), silver nitrate 99.999% (Sigma-Aldrich), and mercuric acetate 99.999% (Sigma-Aldrich) were all high purity and used without additional purification. 0.1 M acetate buffer was prepared by mixing the appropriate amounts of sodium acetate, 99.995% (Sigma-Aldrich), acetic acid, 99.7% (Sigma-Aldrich), calcium acetate, 99.999% (Sigma-Aldrich), and magnesium acetate, 99.999% (Sigma-Aldrich).

The urine simulant contained: ammonium bicarbonate, reagent grade (Columbus Chemical Industries, Columbus, WI), ammonium hydroxide, reagent grade (Columbus Chemical Industries), sodium chloride, 99.7% (Jade Scientific), potassium bicarbonate, 99.7% (Spectrum Chemical, Gardena, CA), creatinine, 98% (Sigma-Aldrich), potassium dihydrogen phosphate, 99% (Sigma-Aldrich), hippuric acid, 99% (Sigma-Aldrich), potassium bisulfate (Sigma-Aldrich), lactic acid, 85%, (Sigma-Aldrich), citric acid, ACS grade (Columbus Chemical Industries), DL-tyrosine, 98% (Sigma-Aldrich), and D-glucuronic acid (Sigma-Aldrich). All chemicals were used without additional purification.

All glassware and nalgene storage bottles were cleaned by a three-step procedure consisting of a thorough washing in an alconox solution, soaking in 1 M hydrochloric acid and 1 M nitric acid for at least 10 min each, and rinsing with ultrapure water. The cleaned glassware was then dried in an oven at ~ 55° C.

2.9. References

(1) Show, Y.; Witek, M. A.; Sonthalia, P.; Swain, G. M. *Chem. Mater.* **2003**, *15*, 879.

(2) Granger, M. C.; Witek, M.; Xu, J.; Wang, J.; Hupert, M.; Hanks, A.; Koppang, M. D.; Butler, J. E.; Lucazeau, G.; Mermoux, M.; Strojek, J. W.; Swain, G. M. *Anal. Chem.* **2000**, *72*, 3793-3804.

(3) Ranganathan, S.; Kuo, T.-C.; McCreery, R. L. *Anal. Chem.* **1999**, *71*, 3574-3580.

(4) Florence, T. M. *J. Electroanal. Chem. Interfacial Electrochem.* **1970**, *27*, 272-281.

(5) McGaw, E.; Sonthalia, P.; Swain, G. M. *SAE Technical Paper 2005-01-2888 35th International Conference on Environmental Systems* **2005**.

(6) NASA. *Simulated Early Planetary Base Mission Wastewater*, **2002**.

CHAPTER 3

COMPARISION OF BORON-DOPED DIAMOND AND Hg-GC WORKING ELECTRODES

3.1. Introduction

Hg based electrodes, drop or thin-film, have been the electrode of choice for ASV for many decades. Hg has many desirable features for this measurement including a large negative potential window, reproducible response, and good sensitivity. However, the toxic and volatile nature of this material are not desirable, and therefore, there is a need for alternative electrode materials with comparable properties. Boron doped diamond (BDD) electrodes have such properties including, a large potential window (negative and positive), a chemically inert surface, a low background current, and a non-toxic and non-volatile nature. These qualities make it a viable alternative to Hg electrodes.

A direct comparison of the performance of BDD and Hg-coated glassy carbon (Hg-GC) electrodes for the detection of Zn^{2+}, Cd^{2+}, Pb^{2+}, Cu^{2+}, and Ag^{+} in standard solutions by ASV was conducted.[1] The basic electrochemical properties of BDD, as they compare with Hg, are described herein. As well as describing the fundamentally different nature of metal deposition and stripping on the two electrode materials, the stripping peak potentials and shapes, and the detection figures of merit for the analytes are presented. The results confirm that BDD is a suitable alternate electrode for ASV that provides comparable or superior detection figures of merit.

3.2. Potential Window

The working potential window is an important characteristic of an electrode used for ASV because it determines which metal ions can be analyzed. For carbon electrodes, the anodic limit in aqueous media is determined by the potential at which oxygen evolution and or electrolyte electrolysis occurs. The cathodic limit is determined by the potential at which hydrogen evolution commences. The kinetic overpotential for these reactions varies depending on the electrode material (i.e., its microstructure and electronic properties). The wide cathodic potential limit for Hg is one of its desirable properties that is difficult to find in alternates. The cathodic limit for Hg extends to -1.3 V (vs. Ag/AgCl) in a pH 4.5 acetate buffer[2]. Only BDD[3] and Bi[4] (another alternate ASV electrode) have cathodic limits this negative. The anodic potential limit, thus the potential window, is also important for multimetal ion analysis. Hg has a working potential window of 1.6 V but, a very low anodic limit.[2] Most other alternate electrodes have more narrow potential windows (e.g., 0.5 V for Au,[5] 1 V for Bi,[4] 0.7 V for Ag[6]) except for BDD, which has a 3 V window.[3] The cathodic limit for BDD is just as negative as that for Hg but the anodic limit of BDD is nearly 2 V more positive. This means that in addition to all of the metal ions Hg can be used to analyze, BDD can also be used for metal ions with $E^{0'}$ values more positive than that for Hg^{2+}/Hg (e.g., Hg^{2+} and Ag^{+}).

3.3. Differential Pulse Anodic Stripping Voltammetry

Standard solutions of Zn^{2+}, Cd^{2+}, Pb^{2+}, Cu^{2+}, and Ag^{+} were used to compare the ASV responses of BDD and Hg-GC. The same conditions were

used for deposition and stripping so that direct comparison of the detection figures of merit for both electrodes could be made. Figure 3.1 shows overlaid stripping voltammetric *i-E* curves for solutions of each individual metal ion.

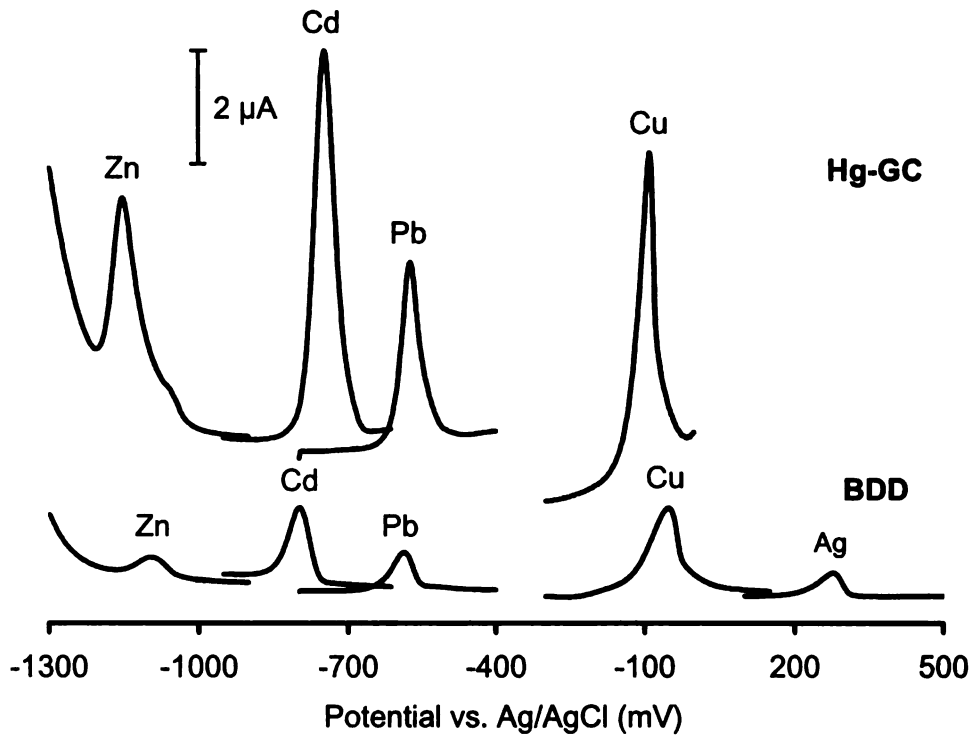

Figure 3.1. Overlaid individual stripping voltammetric *i-E* curves for 100 ppb solutions of each metal ion in 0.1 M acetate buffer, pH 5.2, 30 ppm Ca^{2+}, and 5 ppm Mg^{2+}. The top set of voltammetric *i-E* curves were obtained with Hg-GC and the bottom set with BDD. The curves are offset for clarity. All curves are uncorrected for the background current except the one for Cu on Hg-GC. Figure reprinted with permission from Elsevier.[1]

The oxidation potential for Ag is positive of that for Hg so this metal ion cannot be analyzed using Hg-GC. Well defined stripping peaks are seen for all of the metals using both electrodes, although the peak current and charge (area) for diamond are lower than Hg-GC. A summary of the stripping peak potentials (E_p^{ox}) for both electrodes is presented in Table 3.1, which also includes the

equilibrium potential, E_{eq} for the M^{n+}/M couple, as calculated from the standard reduction potential using the Nernst equation, corrected for the reference electrode (Ag/AgCl), and metal ion activity. The activity coefficients were calculated with the extended Debye-Hückel equation.[7] The activity of the reduced metal phase on BDD is unity because the metal is a pure substance. In the case of the Hg electrode the activity of the reduced metal phase was approximated as unity for these calculations. The reproducibility of E_p^{ox} for both electrodes was comparable. For all the metals, E_p^{ox} for both electrodes was approximately the same, within 70 mV, even for the more electronegative metals. This means that the BDD surface was just as active for the metal phase oxidation as was Hg.

Given that the $E^{0'}$ values for Zn^{2+}/Zn, Cd^{2+}/Cd, and Pb^{2+}/Pb are well negative of the flat band potential for hydrogen-terminated boron-doped (semiconducting) diamond, the voltammetric data indicate that BDD is sufficiently doped to be degenerate electronically.[8, 9] In other words, the electrode exhibits metallic-like electrochemical behavior over a wide potential range.

Table 3.1. Stripping peak potentials and peak widths (FWHM) for BDD and Hg-GC electrodes in the presence of individual metal ions at a 100 ppb concentration are displayed. Mean and standard deviation values (n=3) are presented.

Metal Ion	E_p^{ox} (mV)			FWHM (mV)	
	BDD	Hg-GC	E_{eq}	BDD	Hg-GC
Ag^+	279 ± 4	-	239	59 ± 3	-
Cu^{2+}	-47 ± 3	-84 ± 0	-40	60 ± 3	32 ± 1
Pb^{2+}	-569 ± 1	-554 ± 0	-521	49 ± 2	41 ± 1
Cd^{2+}	-789 ± 1	-732 ± 2	-790	50 ± 2	48 ± 1
Zn^{2+}	-1077 ± 4	-1147 ± 0	-1143	60 ± 1	49 ± 1

The Cd stripping peak for BDD occurs about 50 mV negative of the peak for Hg-GC; however, the standard reduction potential for the Cd^{2+}/Cd couple is approximately 50 mV more negative of that for the $Cd^{2+}/Cd(Hg)$ reaction.[10] This accounts for the difference in E_p^{ox} for the two electrodes. In the case of Zn, E_p^{ox} is near the predicted value for Hg-GC, however, for BDD the value is 65 mV more positive. This suggests that there is a slight overpotential for this reaction on BDD. There is also a difference in E_p^{ox} for Cu for the two electrodes. E_p^{ox} for Hg-GC is approximately 45 mV more negative than the calculated E_{eq}. There is a small difference of 5 mV between the standard reduction potential for the Cu^{2+}/Cu and $Cu^{2+}/Cu(Hg)$, so this does not account for the difference.[10] In fact, Hg-GC displayed very unusual behavior in the potential region of Cu stripping, which likely affects E_p^{ox}. A very broad peak centered about 0 mV vs. Ag/AgCl was observed in the background. An overlay of the background and total voltammetric stripping current for a phase formed from a 100 ppb Cu^{2+} solution at both Hg-GC and BDD is presented in Figure 3.2.

The shape, position, and magnitude of this background peak on Hg-GC did not vary with the Hg^{2+} solution concentration, and it was present at the same magnitude even when no Hg^{2+} was present. This confirms that the oxidation peak is not caused by Hg or a contaminant in the Hg^{2+} salt. Further investigation by cyclic voltammetry revealed that the peak height varied linearly (r^2 = 0.997) with scan rate between 20 and 300 mV/s. This trend is consistent with an oxidation reaction involving a surface confined molecule. The peak potential also shifted by -54 mV/pH (r^2 = 0.999) as the pH of the buffer was varied from 3.0 to

5.2. This is very close to the theoretical -59 mV/pH slope predicted by the Nernst equation for a reaction involving equal numbers of H^+ and e^-. Based on these data, the background peak was ascribed to hydroquinone functionalities on the GC surface that are oxidized to the corresponding quinone at this potential. As expected, this peak is not seen in the voltammetric *i-E* curves for BDD because such functionalities do not exist on the hydrogen-terminated surface. The presence of the peak in the Hg-GC background complicated the analysis for Cu^{2+} making background subtraction necessary for quantitation. It is supposed that the oxidation of the underlying carbon simultaneously with the oxidation of the solid Cu phase causes the apparent shift in E_p^{ox}.

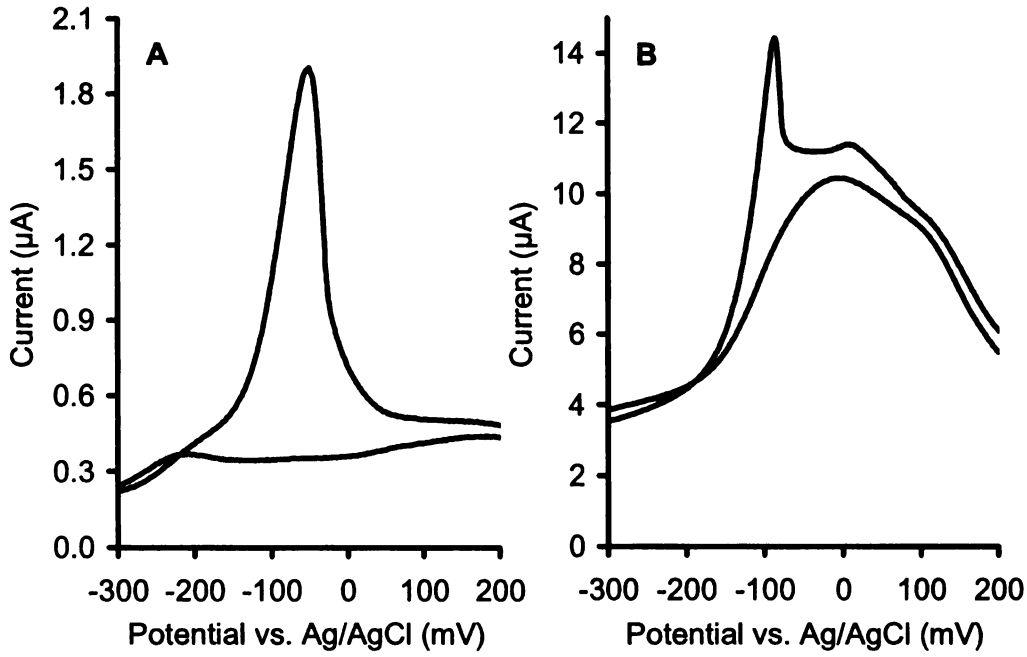

Figure 3.2. Differential pulse stripping voltammetric *i-E* curves for 100 ppb Cu^{2+} in 0.1 M acetate buffer, pH 5.2. 30 ppm Ca^{2+} and 5 ppm Mg^{2+} were added. The background voltammetric *i-E* curves are also shown for comparison. The deposition potential was -400 mV vs. Ag/AgCl and the deposition time was 210 s. The working electrodes were BDD (A) and Hg-GC (B). Note the difference in current scales. Figure reprinted with permission from Elsevier.[1]

Another important parameter is the stripping peak width, which is assessed by the width at half height (FWHM). Analytically, narrow peaks are desired to improve the resolution of the measurement, thereby enabling the detection of metal ions with closely spaced formal potentials. In Table 3.1, a summary of the FWHM values for each metal at both electrodes is presented. Both electrodes show similar FWHM values for all the metals, with the values for BDD being slightly higher.

The broader peaks for BDD are attributed to the heterogeneous nature of the electrical and electrochemical properties across the surface.[11] The Hg environment is simply more chemically and electrically homogeneous than is the polycrystalline diamond surface. In other words, metal phase oxidation from Hg occurs with one apparent heterogeneous electron-transfer rate constant, while the oxidation from BDD likely occurs with a variable rate constant, depending on the particular location on the surface. Moreover, the peak widths for BDD are also influenced by the morphology of the metal deposit. For BDD or any alternate electrode, a uniformly dispersed metal phase of small nominal particle size and narrow size distribution is desired.[12] The dc deposition condition used in the present work produced metal deposits of varying size (volume) on BDD, far from optimum.[3, 12] This coupled with the heterogeneous chemical and electrical properties inherently lead to broader stripping peaks than are seen for Hg-GC. Even with this heterogeneity, the peak widths for BDD are not excessively broad such that they preclude the analysis of multiple metal ions.

In addition to the broader peaks, there is a difference in peak shapes for the two electrodes (Figure 3.3). The *i-E* curves for Hg-GC are more symmetric in shape than are those for BDD, the latter being asymmetric with peak fronting. The shape differences likely occur because of the manner in which the metal phase is formed and subsequently oxidized at each electrode. In the case of Hg, foreign metals deposit within a volume of Hg to form an amalgam. Thus, the analyte metal resides in a very homogeneous environment with the concentration of metal being proportioned to the volume of the Hg present. Because of this chemical and electrical homogeneity, the oxidation reaction kinetics are uniform for all metal atoms giving rise to a symmetric peak shape. However, metal deposition on BDD occurs in a completely different manner. The metal deposits form on the surface as particles with some metal atoms having only metal-metal interactions and others having metal-diamond interactions. The polycrystalline nature of BDD, in terms of the site heterogeneity and the non-uniform electrical conductivity, makes for a complex surface from which metal oxidation occurs.[11] It is expected that at slower scan rates the effect of the surface heterogeneity would be minimized and the peaks would be more symmetric. In fact symmetric peaks were observed on BDD for scan rates < 5 mV/s, which is consistent with the complex surface leading to the asymmetric peak shape.

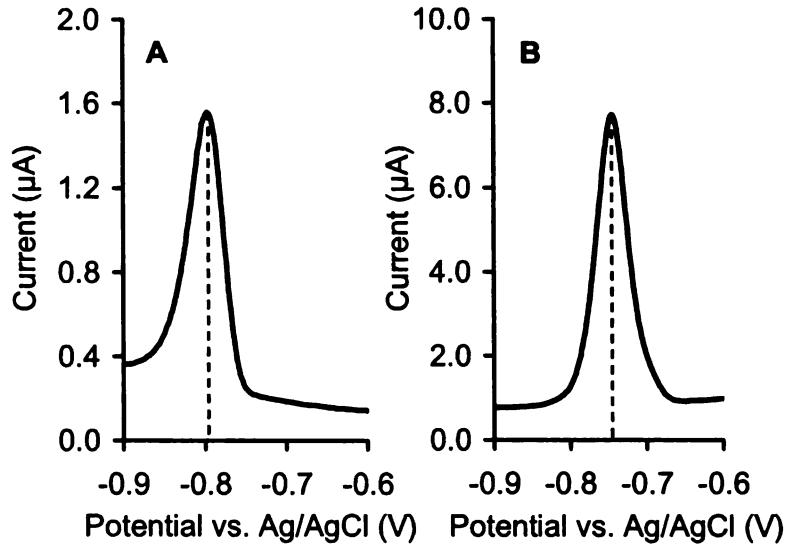

Figure 3.3. Differential pulse stripping voltammetric *i-E* curves for 100 ppb Cd^{2+} in 0.1 M acetate buffer, pH 5.2, 30 ppm Ca^{2+}, and 5 ppm Mg^{2+}. The deposition potential was -400 mV vs. Ag/AgCl and the deposition time was 210 s. The working electrodes were BDD (A) and Hg-GC (B). Note the difference in current scales.

The rising portion of the *i-E* curves for Cd, Pb, and Cu on Hg-GC can be fit to an exponential trend ($r^2 \geq 0.997$), and the peak occurs near the theoretically predicted potential. Such shape is consistent with fast oxidation reaction kinetics, and an apparent rate constant that is the same across the surface. Oxidation of the metal phase is an exhaustive electrolysis process (pseudo thin-layer behavior) so that the peaks tend to be relatively narrow with no diffusional tail past the maximum. As long as the Hg volumes from which the metal phase is being oxidized are relatively constant across the surface, the peak widths will be narrow, approaching the theoretical value 45.3 mV (n=2).[13] On the other hand, the rising portion of the *i-E* curve on BDD increased more slowly with potential, and could not be accurately described by an exponential function. As discussed

above, there are many different surface sites (chemically and electrically) from which metal phases can be oxidized. This site variability leads to drawn out *i-E* curves. Even though the BDD peaks have a different shape, overall both electrodes yielded similar responses in terms of peak position and width. The similarity of these parameters indicates the metal oxidation reactions are nearly as favorable for BDD as they are for Hg.

3.4. Detection Figures of Merit

Despite the lower stripping peak current and charge (area) for all the metal ions, the limit of detection and linear dynamic range for BDD are practically the same as for Hg-GC. Figure 3.4 presents a series of stripping voltammetric *i-E* curves for standard solutions of Cd^{2+} at BDD and Hg-GC. For both electrodes, the current and charge increase proportionally with the solution concentration. However, the slopes of the response curves for Hg-GC are about a factor of four higher than those for BDD. A summary of the metal ion analysis data is presented in Table 3.2. The peak current and charge data presented were background corrected. The background current values reported were measured at the stripping peak potential for each metal. In all cases, the background current for BDD was lower than that for Hg-GC by a factor of three to ten. This is especially apparent for the more electronegative metals, Cd^{2+} and Zn^{2+}. A characteristic property of BDD is a low and featureless background current that is stable with potential and time.[3, 14] The background current for Hg-GC depends on the condition of the GC surface as well as the amount of Hg present but, in general, is a factor of 5-10 greater than for BDD of the same geometric area.

The lower background current leads to enhanced signal-to-background ratios in electroanalytical measurements. Additionally the peak-to-peak fluctuation (noise) in the background current is lower for BDD.

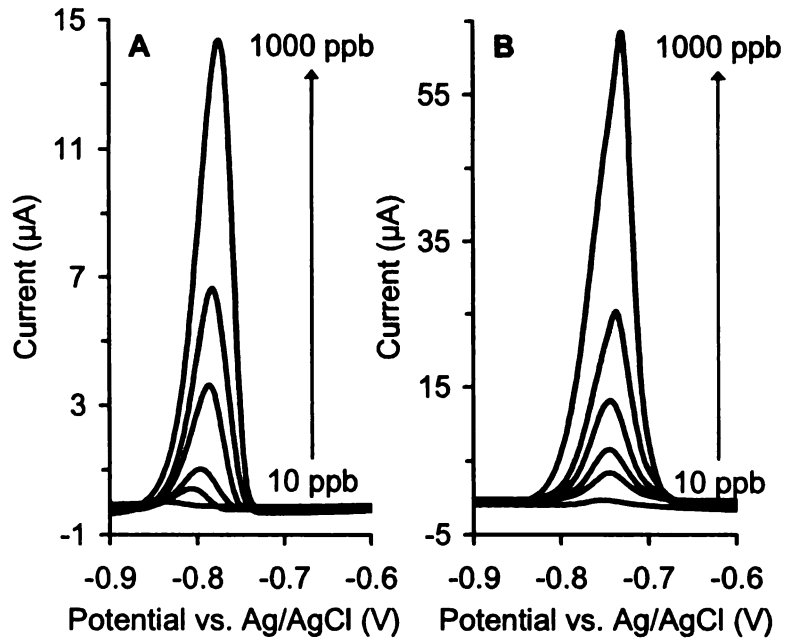

Figure 3.4. Differential pulse stripping voltammetric *i-E* curves for standard solutions of Cd^{2+} in 0.1 M acetate buffer, pH 5.2, 30 ppm Ca^{2+}, and 5 ppm Mg^{2+}. The deposition potential was -1000 mV vs. Ag/AgCl and the deposition time was 210 s. The working electrodes were BDD (A) and Hg-GC (B). Note the difference in current scales. Figure reprinted with permission from Elsevier.[1]

The minimum concentrations detectable at signal-to-noise ratio (S/N) ≥ 3 are also presented in Table 3.2. For Cd^{2+}, Pb^{2+}, Cu^{2+}, and Ag^{+}, concentrations from 1 – 10 ppb were detectable with BDD. These values are as good or superior to the values for Hg-GC. Ag^{+} was detectable down to a level of 1 ppb but only with BDD. The minimum concentration of Zn^{2+} detectable with BDD was a factor of five higher than with Hg-GC. The exact reason for this is unknown but may have to do with the electronic properties of the electrode at the stripping

potential. There is also a discrepancy between the minimum concentrations of Cu^{2+} detectable with the two electrodes. The lowest concentration detectable with BDD is a factor of five lower than the value for Hg-GC. As discussed previously, the large background signal from the redox-active carbon-oxygen functionalities on GC complicate the analysis of Cu^{2+}. The magnitude of this background peak is in the μA range, making it difficult to separate from the Cu^{2+} signals, and impossible to obtain a low detection limit.

The sensitivity is an important parameter for low detection limits. Hg-GC exhibits a response sensitivity that is three to five times greater than BDD for each of the metal ions. Typically, a higher sensitivity value will result in a lower limit of detection, which is seen in equation 3.1

$$C_{LOD} = \frac{3N}{m} \tag{3.1}$$

C_{LOD} is the minimum concentration detectable (ppb), N is the amplitude of the noise (A) and m is the sensitivity of the measurement (A/ppb). Even though the sensitivity was lower for BDD, the lower noise/background current enabled as good or superior C_{LOD} values to be achieved. While a direct comparison of the sensitivity is often useful for determining how well two electrodes perform analytically, it is not a good comparative of these two electrodes.

Table 3.2. Detection figures of merit for metal ions measured using BDD and Hg-GC electrodes.

		Background at Peak Potential (μA)	Lowest Concentration Detected (ppb) S/N ≥ 3	Sensitivity (nA/ppb)	Linear Dynamic Range (ppb)	Reproducibility (RSD at 250 ppb n=3)
Zn^{2+}	BDD	0.7 ± 0.1	50	9.48 ± 0.20	50 - 1000*	4.8%
	Hg-GC	2.5 ± 0.6	10	46.5 ± 1.5	10 - 1000*	0.8%
Cd^{2+}	BDD	0.47 ± 0.05	1.0	14.7 ± 0.2	1 - 1000*	3.1%
	Hg-GC	1.7 ± 0.7	1.0	62.0 ± 2.9	1 - 1000*	7.6%
Pb^{2+}	BDD	0.33 ± 0.09	5.0	13.0 ± 0.4	5 - 1000*	3.8%
	Hg-GC	1.2 ± 0.2	5.0	34.9 ± 1.4	5 - 1000*	3.6%
Cu^{2+}	BDD	0.36 ± 0.01	10	7.14 ± 0.41	10 - 1000*	1.1%
	Hg-GC	12 ± 3	50	31.4 ± 3.9	50 - 1000*	3.2%
Ag^{+}	BDD	0.24 ± 0.07	1.0	9.12 ± 0.18	1 - 1000*	3.4%
	Hg-GC	-	-	-	-	-

* Denotes largest concentration measured and is not necessarily the upper limit

Another important analytical parameter to compare is the linear dynamic range, which is assessed from response curves. The response curves were linear for all metal ions at both electrodes from the low to the high (1000) ppb range with linear regression correlation coefficients of 0.99, or greater. Previous studies have shown that BDD provides a linear dynamic range of four orders of magnitude for various metal ions.[3] This range is comparable with that for Hg-GC, and is more than adequate for most analytical applications. Lastly, BDD must have the same reproducibility of results as a Hg-based electrode. For all of the metals tested, BDD showed a run-to-run variability of less than 5 % RSD (n=3), and this is comparable to values for Hg-GC. However, if BDD is to be a viable alternate electrode, reproducible results must also be obtained from electrode-to-electrode. This was assessed by analyzing a 100 ppb Ag^+ solution with four different films using a minimum of three measurements for each. It was found that the electrode-to-electrode reproducibility was excellent with a variability of only 3.8% RSD.

3.5. Comparison of Metal Deposition and Stripping Charge for BDD

In past studies with BDD, issues with both incomplete metal oxidation and metal phase detachment have been reported, both of which limit the response sensitivity in ASV.[15-17] No evidence for metal phase detachment during past work with Pt electrodeposition on BDD was observed.[18-20] Since the ASV analysis involves different metal phases, a few experiments were conducted to probe for metal loss by either incomplete oxidation or detachment.

The first set of experiments was designed to look for incomplete metal oxidation. Double potential step chronoamperometry was used to record the current passed as a function of time during the deposition and stripping steps. The *i-t* curves were integrated to determine the charge passed. The first step was to apply 0.6 V for 3 min to oxidize any remnant metal particles from previous measurements. Following this, the metal particles were formed via electrodeposition at a potential for which the reaction is mass transfer limited. This potential was different for each metal, depending on its $E^{o'}$. The deposition time in each case was 210 s. The potential was then switched to 0.6 V for the same period of time to oxidize the metal phase. The apparent faradaic charge for the metal deposition and oxidation were determined by subtracting the background charged recorded in the absence of the analyte metal ion. The resulting data are presented in Table 3.3.

Theoretically, the stripping/deposition charge ratio should be unity if both reactions occur with 100% efficiency. In the case of the electropositive Ag^{+}/Ag couple, the ratio was very near unity. This confirms that incomplete metal phase oxidation did not occur to any appreciable extent on these films, at least for this metal, as has been reported previously.[15, 17] The ratio decreased progressively for the more electronegative metals ranging from 93% for Ag^{+}/Ag to only 8% for Zn^{2+}/Zn. This was because the deposition charge progressively increased with the deposition potential (e.g., Zn and Cd), and it reflects all reactions occurring at the electrode. The more negative the potential is, the more reactions that

Table 3.3. Deposition and stripping charges for individual metal ions at a concentration of 1 ppm in 0.1 M acetate buffer, pH 5.2 using a BDD electrode.

Metal	Zn (E_{dep} = -1.3 V)	Cd (E_{dep} = -1.0 V)	Pb (E_{dep} = -0.8 V)	Cu (E_{dep} = -0.4 V)	Ag (E_{dep} = 0.0 V)
Deposition Charge (μC)	-190 ± 10	-48.5 ± 3.6	-14.6 ± 0.7	-28.3 ± 0.2	-9.38 ± 0.08
RSD	5.0%	7.3%	5.1%	0.63%	0.83%
Stripping Charge (μC)	16.0 ± 0.3	7.86 ± 0.11	2.19 ± 0.06	19.7 ± 0.3	8.70 ± 0.30
RSD	1.8%	1.3%	2.8%	1.7%	3.5%
Charge Ratio (Stripping/Deposition)	0.083 ± 0.005	0.16 ± 0.01	0.15 ± 0.01	0.69 ± 0.01	0.93 ± 0.04
RSD	6.4%	8.5%	6.1%	1.5%	4.35%

A double potential step chronoamperometric experiment was performed using step widths of 210 s, deposition potentials as listed in the table and a stripping potential of 0.6 V. The deposition and stripping current-time profiles were integrated to obtain the deposition and stripping charge. All data are background corrected. Errors listed are calculated from standard deviation of multiple measurements (n=3) taken with a single electrode

are possible. For these particular metals, hydrogen evolution is a key parasitic reaction. While the reaction kinetics are not known for each of the metals it is reasonable to suppose that the hydrogen evolution reaction kinetics are more rapid for all of the metal phases than for diamond. This would account for a greater cathodic charge passed during the deposition step for the more electronegative metals (i.e., the decreasing stripping/deposition charge ratio).

To confirm that the stripping/deposition charge ratio decrease was a function of the deposition potential rather than the property of the specific metals a similar experiment was performed using only Cu^{2+}. The same deposition potentials were used as in the previous experiment, and the results are presented in Table 3.4. From these data the same trend is observed again, a decreasing stripping/deposition charge ratio with decreasing deposition potential, suggesting that this phenomenon is related to parasitic reactions.

A second set of experiments was performed to look for metal phase detachment. Double-potential step chronoamperometry was used to record the current passed as a function of time during deposition and stripping steps. The measurements were made as a function of time with the hypothesis that longer deposition times would lead to more metal phase formation, and consequently, greater detachment. Cu was chosen to probe this effect because detachment of this metal has been previously reported, and the results are summarized in Table 3.5.[16]

As expected, the charge passed increased proportionally with deposition time. The charge ratio basically remained constant (~70%) for all deposition

Table 3.4. Deposition and stripping charges for 1 ppm Cu^{2+} in 0.1 M acetate buffer, pH 5.2 using a BDD electrode, varying deposition potential.

E_{dep} (V)	-1.3	-1.0	-0.8	-0.4
Deposition Charge (μC)	-25200 ± 450	-1540 ± 39	-127 ± 2	-28.7 ± 0.7
RSD	1.79%	2.51%	1.27%	2.55%
Stripping Charge (μC)	82.5 ± 1.3	27.8 ± 0.3	24.7± 0.7	23.4 ± 0.8
RSD	1.53%	1.18%	2.64%	3.56%
Charge Ratio (Stripping/Deposition)	0.00327 ± 0.00002	0.0180 ± 0.0002	0.194 ± 0.003	0.82 ± 0.05
RSD	0.58%	1.33%	1.47%	5.83%

A double potential step chronoamperometric experiment was performed using step widths of 210 s, deposition potentials as listed in the table and a stripping potential of 0.6 V. The deposition and stripping current-time profiles were integrated to obtain the deposition and stripping charge. All data are background corrected. Errors listed are calculated from standard deviation of multiple measurements (n=3) taken with a single electrode

Table 3.5. Deposition and stripping charges for 1 ppm Cu^{2+} in 0.1 M acetate buffer, pH 5.2 using a BDD electrode, varying deposition time.

Deposition Time	5 s	10 s	30 s	60 s	210 s
Deposition Charge (μC)	-3.12 ± 0.03	-4.66 ± 0.01	-8.83 ± 0.26	-12.8 ± 0.1	-28.3 ± 0.2
RSD	0.88%	0.27%	1.8%	0.74%	0.63%
Stripping Charge (μC)	1.08 ± 0.01	2.65 ± 0.01	6.16 ± 0.03	9.34 ± 0.02	19.7 ± 0.3
RSD	0.94%	0.54%	0.44%	0.22%	1.7%
Charge Ratio (Stripping/Deposition)	0.35 ± 0.003	0.57 ± 0.002	0.70 ± 0.01	0.73 ± 0.004	0.69 ± 0.01
RSD	0.74%	0.44%	1.4%	0.59%	1.5%

A double potential step chronoamperometric experiment was performed with varying deposition time. The deposition potential was -0.4 V and the stripping potential was 0.6 V. The current-time profiles were integrated to obtain the deposition and stripping charge. All data were background corrected. Errors listed are calculated from the standard deviation of multiple measurements (n=3) taken with a single electrode

times except the shortest, for which there was a significant decrease. The fact that the stable ratio is less than 100% is attributed to the parasitic evolution of hydrogen on the depositing metal phase. The relatively constant ratio is evidence for minimal metal phase detachment. The trend in the stripping/deposition charge ratio with deposition time is consistent with a metal formation and growth model.[21] In this model, metal phase formation involves nucleation of a metal phase and growth of the deposit from the initially formed nuclei. The nuclei must reach some critical size before they become stable on the surface and then function as sites for growth. Sufficiently long deposition times (i.e., induction time) are needed to achieve the critical size. At the short deposition times (e.g., 5 s and 10 s), the efficiency of the deposition is not as high as at long times because few of the nuclei reach critical size (i.e. are stable). Experimentally, this same trend was observed by Hyde et al. in a study of Ag electrodeposition on BDD. They noted a 15 s "induction period" during which few nuclei formed on the surface.[22]

3.6. Conclusions

It was shown through direct comparison measurements that BDD is a suitable alternative electrode to Hg for the ASV determination of common metal ion contaminants. BDD exhibits many of the same electrode properties as does Hg, but it is not toxic or volatile. BDD also has a wider anodic potential limit, and a lower background current density than Hg. Due to the hydrophobic nature of the hydrogen-terminated surface, BDD is quite resistive to deactivation such that conventional time-consuming pretreatment is normally not needed. This is an

attractive feature for real sample analysis. Overall, the detection figures of merit for BDD are as good or superior to those for Hg-GC. Both BDD and Hg-GC provided detection limits for all the metal ions in the mid to low ppb range (S/N ≥ 3). Only the minimum detectable concentration for Zn^{2+} was lower for Hg-GC. The response reproducibility was < 5% (RSD) for BDD from run-to-run and from electrode-to-electrode. The biggest difference between the two electrodes is the magnitude of the stripping peak current and charge, which are greater for Hg-GC. The larger electrochemical response on Hg-GC resulted in a higher sensitivity, but this was offset by a similar reduction in the background noise for BDD which resulted in comparable or lower C_{LOD} values. Electrochemical measurements revealed that reduced sensitivity due to incomplete metal oxidation or metal phase detachment was not an issue for these BDD films.

3.7. References

(1) McGaw, E.; Swain, G. M. *Anal. Chim. Acta* **2006**, *575*, 180-189.

(2) Wang, J.; Lu, J.; Hocevar, S. B.; Farias, P. A. M.; Ogorevc, B. *Anal. Chem.* **2000**, *72*, 3218-3222.

(3) Show, Y.; Witek, M. A.; Sonthalia, P.; Swain, G. M. *Chem. Mater.* **2003**, *15*, 879.

(4) Chatzitheodorou, E.; Economou, A.; Voulgaropoulos, A. *Electroanal.* **2004**, *16*, 1745-1754.

(5) Bonfil, Y.; Brand, M.; Kirowa-Eisner, E. *Anal. Chim. Acta* **1999**, *387*, 85-95.

(6) Kirowa-Eisner, E.; Brand, M.; Tzur, D. *Anal. Chim. Acta* **1999**, *385*, 325-335.

(7) Debye, P.; Huckel, E. *Physik. Z.* **1923**, *24*.

(8) Swain, G. M.; Ramesham, R. *Anal. Chem.* **1993**, *65*, 345-351.

(9) Alehashem, S.; Chambers, F.; Strojek, J. W.; Swain, G. M.; Ramesham, R. *Anal. Chem.* **1995**, *67*, 2812-2821.

(10) Bard, A. J.; Faulkner, L. R. *Electrochemical Methods Fundamentals and Applications*, 2nd ed.; John Wiley & Sons, Inc.: New York, NY, 2001.

(11) Holt, K. B.; Bard, A. J.; Show, Y.; Swain, G. M. *J. Phys. Chem. B* **2004**, *108*, 15117-15127.

(12) Sonthalia, P.; McGaw, E.; Swain, G. M. *Anal. Chim. Acta* **2004**, *522*, 35-44.

(13) Ramaley, L.; Krause Jr., M. S. *Anal. Chem.* **1969**, *41*, 1362-1365.

(14) Granger, M. C.; Witek, M.; Xu, J.; Wang, J.; Hupert, M.; Hanks, A.; Koppang, M. D.; Butler, J. E.; Lucazeau, G.; Mermoux, M.; Strojek, J. W.; Swain, G. M. *Anal. Chem.* **2000**, *72*, 3793-3804.

(15) Vinokur, N.; Miller, B.; Avyigal, Y.; Kalish, R. *J. Electrochem. Soc.* **1999**, *146*, 125-130.

(16) Nakabayashi, S.; Tryk, D. A.; Fujishima, A.; Ohta, N. *Chem. Phys. Lett.* **1999**, *300*, 409-413.

(17) Awada, M.; Strojek, J. W.; Swain, G. M. *J. Electrochem. Soc.* **1995**, *142*, L42-L45.

(18) Wang, J.; Swain, G. M. *Electrochem. Solid-State Lett.* **2002**, *5*, E4-E7.

(19) Wang, J.; Swain, G. M. *J. Electrochem. Soc.* **2003**, *150*, E24-E32.

(20) Bennett, J. A.; Show, Y.; Swain, G. M. *J. Electrochem. Soc.* **2005**, *152*, E184-E192.

(21) Pletcher, D. *A First Course in Electrode Processes*; Alresford Press Ltd.: Alresford, Great Britain, 1991.

(22) Hyde, M. E.; Jacobs, R. M. J.; Compton, R. G. *J. Electroanal. Chem.* **2004**, *562*, 61-72.

CHAPTER 4

METHOD ADJUSTMENTS FOR MICROGRAVITY APPLICATION

4.1. Introduction

Water on-board the International Space Station (ISS) presently comes from three sources: recovered humidity condensate, fuel cell transfer water from the Shuttle, and preparations on earth.[1-3] A large portion of the crew's drinking water is supplied from the condensate (recovered water), which is treated in and dispensed from the SRV-K system. The resulting deionized water is then passed through a conditioning bed that adds 300-500 ppb of Ag^+ for biocidal purposes and minerals (calcium, magnesium, and fluoride ions) for taste. The water is then pumped to a galley where it is pasteurized and dispensed. The water from the SRV-K system is not prepared for extended storage but rather is supplied on demand.

The remaining supply comes from the stored water, which is mainly the Shuttle fuel cell transfer water. Iodine is added to this stored water at a concentration of 2-4 ppm for biocidal purposes. This water is prepared for transfer to ISS by first deiodinating it, and then storing it in contingency water containers (CWCs, 44 L). As water is being collected in the CWC, Ag^+ is added (300-500 ppb) along with minerals for taste. These chemicals are added during the collection process from ground-loaded syringes to ensure homogeneous mixing.[2] This stored water, referred to as potable, is transferred to ISS in the CWC, and is used for drinking, food rehydration, and hygiene. It can be dispensed directly from a CWC using the SVO-ZV system. Some of the fuel cell

water is also prepared for transfer by adding Ag^+ without any mineralization. This water is referred to as technical, and is used mainly for toilet flushing and electrolytic oxygen generation. In the event that the volume of recovered water available does not meet the crew demand, the potable water can be added to the SRV-K system – so-called make-up water.

The water quality is a critical issue for crew health and safety. There is presently minimal monitoring capability of the recovered and stored water on-board ISS. Therefore, there are no means for rapidly responding to a contamination event. Monitoring of the ISS water is currently performed by periodically collecting (~1 month intervals) both SRV-K and SVO-ZV water in special Teflon storage bags.[1-3] These samples are then returned to earth during resupply expeditions, and comprehensively analyzed for turbidity, pH, organic and inorganic chemical content, and biological agents. Ag^+, of course, is important to regularly monitor in both the recovered and stored water in order to assess biocidal activity. Additionally, other metal ion contaminants have been detected in water samples returned from previous Shuttle expeditions.[1, 3] For example, Pb^{2+} levels near or above the Environmental Protection Agency (EPA) action limit of 15 ppb and Cd^{2+} levels above NASA's Medical Operations Requirement Document (MORD) limit of 5 ppb have been found. The sources of these contaminants have been identified, and system corrections made to eliminate them. However, the unexpected appearance of these toxic inorganic contaminants points to the need for on-board monitoring and control.

The requirements for an analytical technique suitable for space applications are different from those needed on earth. First of all, the instrumentation must be lightweight, compact, robust, and energy efficient. The technique must have long-term stability, as replenishing missions are several months apart, and require little user interaction. Furthermore, there are limitations because of the microgravity environment. All liquids must be enclosed and, for safety reasons, the pH range is limited to between 5.5 and 9.

Electrochemical methods are attractive for on-board monitoring because they fulfill many of these requirements. Electrochemical methods require minimal maintenance and user interaction especially, if a stable and sensitive electrode material is employed. The goal of this work was to develop an electrochemical method for water quality monitoring using a boron-doped diamond thin film (BDD) electrode and anodic stripping voltammetry (ASV).[4] The focus was on heavy metal ions (e.g., Ag^+ biocide).

Due to the stringent requirements on-board, work was conducted to adapt a previously developed ground-based method. Efforts to evaluate the ASV method (i) at increased pH from 4.5 to 5.2, (ii) after adding Ca^{2+} and Mg^{2+} salts for mineralization, (iii) after eliminating the nitrogen purge step (dissolved oxygen removal), and (iv) during long-term electrode response stability, are reported. Additionally, the development of a prototype microgravity cell, and results from the analysis of Ag^+ in simulated potable and technical water samples, provided by the Wyle Laboratory (Johnson Space Center) are discussed.

4.2. Solution Parameters

4.2.1. Effect of pH Adjustment

Ground-based ASV methods are usually performed in an acetate buffer supporting electrolyte solution at pH 4.5.[5, 6] The pH of this solution is outside the range allowable for use on-board ISS (5.5 to 9). Tests were therefore conducted to determine the detection figures of merit for Ag^{+}, Cu^{2+}, Pb^{2+}, Cd^{2+}, and Zn^{2+} in an acetate buffer supporting electrolyte solution at pH 5.2.

Increasing the solution pH can have two harmful effects on metal ion analysis by ASV. First, the activity of a metal ion can be reduced due the formation of metal hydroxide species (soluble and insoluble). Second, the increase in pH shifts the onset for hydrogen evolution toward more positive potentials, and this can interfere with the detection of metal ions having very negative standard reduction potentials (e.g., Zn^{2+}). Table 4.1 shows the minimum concentration of each metal ion detected along with the S/N ratio at pH 5.2, and comparison data at pH 4.5 are also presented. It should be noted that the measurements at pH 4.5 were made using a pulse height of 100 mV while the measurements at pH 5.2 were made with a pulse height of 50 mV. The decrease in pulse height may slightly decrease the response sensitivity by reducing the stripping peak current. However, the choice was made to use the more standard 50 mV pulse height because no significant improvement was seen using larger pulse heights.[7, 8]

Even with the different voltammetric parameters, and the solution pH increase, the minimum detectable concentrations for Cd^{2+}, Pb^{2+}, and Cu^{2+},

measured or estimated for a S/N of 3, are in the low ppb range. The exceptions are Zn^{2+} and Ag^{+}. The higher minimum detection for Zn^{2+} at the higher pH is expected do to the greater interference by hydrogen evolution on Zn metal formation during the deposition step. The data for Ag^{+} reveals that the minimum detectable concentration is a factor of 10 higher at pH 5.2. This was an unexpected result but it may be caused by the formation of Ag^{+} acetate complexes, which would reduce the Ag^{+} activity in solution. There are two known Ag acetate (OAc) complexes: AgOAc and $Ag(OAc)_2^-$. Using complexation equilibrium equations and mass balances in the pH range of 4 to 6 there is a 2% decrease in the amount of free Ag^{+} when OAc is present. Even at pH 5.2, the detection limit for Ag^{+} is still in the low ppb range, well below the MORD required limit of 50 ppb.

Table 4.1. Comparison of the minimum concentrations of several priority metal ions detectable with a diamond thin-film electrode at pH 4.5 and pH 5.2.

Metal Ion	**pH 4.5**		**pH 5.2**	
	ppb	S/N	ppb	S/N
Zn^{2+}	6.5	3	50	20
Cd^{2+}	1.1	5	10	30
Pb^{2+}	2.1	3	5.0	3
Cu^{2+}	0.64	3	10	20
Ag^{+}	0.11	4	1.0	4

In terms of the response sensitivity, the effect of increasing the pH appears minimal for all the metal ions except Zn^{2+}. For example, the response sensitivity for Ag^{+} was 110 nC/ppb at pH 4.5 and 130 nC/ppb at 5.2.

4.2.2. Effect of Mineralization

Ca^{2+} and Mg^{2+} formate salts are added to the SRV-K water for taste at concentrations of 30 and 5 ppm, respectively. Measurements were conducted to determine if the presence of the salts affected the electrochemical response of standard solutions of the metal ions. In this study, acetate salts of Ca^{2+} and Mg^{2+} were used instead of the formate salts used in NASA preparations of potable water.

Table 4.2. Comparison of the stripping response (peak area) for each priority metal ion before and after the addition of Ca^{2+} and Mg^{2+} salts.

Metal Ion	Peak Area (μC)		% Difference
	Salt	No Salt	
100 ppb Zn^{2+}	0.66	0.69	-3.8
50 ppb Cd^{2+}	0.86	0.85	0.92
100 ppb Pb^{2+}	1.9	1.9	-0.24
500 ppb Ag^{+}	3.9	3.8	3.0

The addition of these cations has little effect on the ASV response for any of the priority metal ions. Less than a 4% change was observed.

4.2.3. Effect of Dissolved Oxygen

Solutions are normally purged of dissolved oxygen prior to making an ASV measurement. The reduction of oxygen both at the BDD surface and the deposited metal surface compete with metal deposition during the preconcentration step. This may reduce the amount of metal formation resulting in decreased stripping current. On earth the removal of oxygen is usually accomplished by sparging the solution with an inert gas (e.g., N_2, Ar). Oxygen removal with this method is not possible on-board ISS so the effect of dissolved oxygen on the diamond thin-film electrode response for each of the priority metal

ions was investigated. Standard solutions containing the metal ions (Cd^{2+}, Pb^{2+}, Cu^{2+}, and Ag^{+}) were tested individually, both with and without a 3 min N_2 purge. All measurements were made in acetate buffer, pH 5.2.

The presence of dissolved oxygen did not significantly affect the ASV response for Ag^{+} or Cd^{2+} at BDD, as demonstrated for Ag^{+} in Figure 4.1 A. The stripping peak potential, current, and charge (area) were unchanged in the presence of dissolved O_2. The only difference between the Ag^{+} and Cd^{2+} responses was the higher background current without an N_2 purge at potentials where Cd is detected. However, the faradaic current for Cd^{2+} stripping was not affected. This higher background was due to the O_2 reduction reaction that occurs in the potential range where the Cd is oxidized (stripped).

On the other hand, there was a significant effect on the stripping peak for Pb^{2+} as shown in Figure 4.1 B. It is clear that when dissolved oxygen is present, the stripping peak current and charge are reduced. There is also a small reduction in the signal from Cu^{2+} (~15%) when dissolved oxygen is present. The effect is not related to the E^0 of the metals because Cd was not affected, and it has a more negative E^0 than either Pb or Cu. It is thought that the reason only these two metal ions were affected by the dissolved O_2 has to do with their reactivity with oxygen. There are two possible causes for this effect. First, the deposited Pb (solid) could react with oxygen to make PbO_2, passivating the surface and inhibiting the oxidation. Second, reactive oxygen species (e.g., H_2O_2, $O^{\bullet}$) could chemically oxidize the deposited Pb from the surface, removing it prior to electrochemical oxidation.

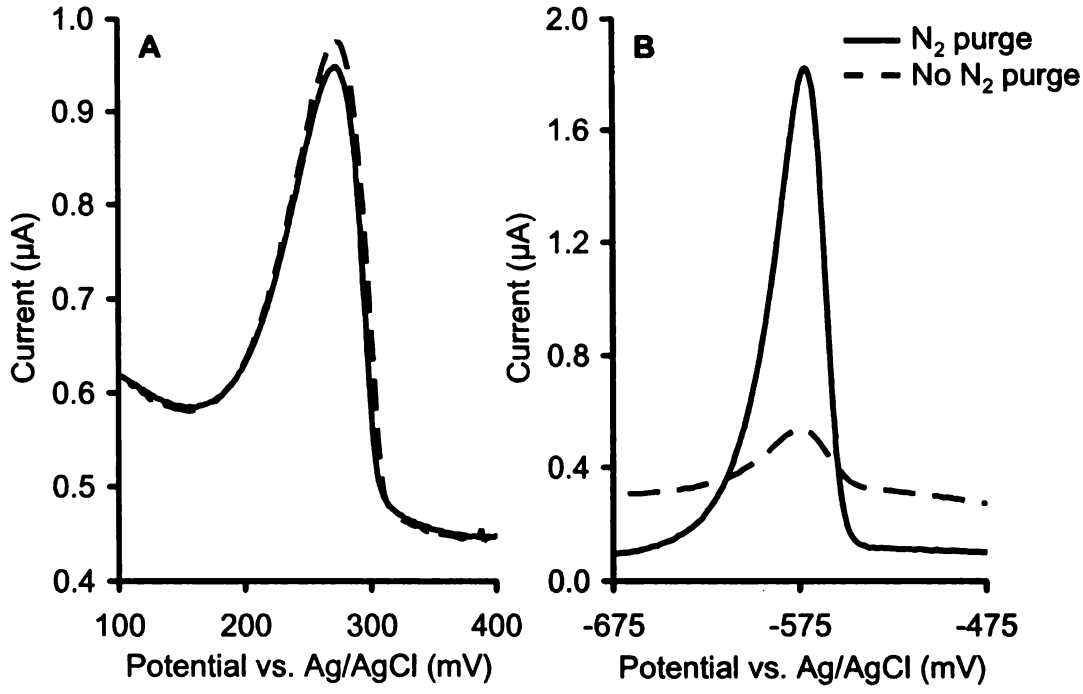

Figure 4.1. Stripping voltammetric *i-E* curves for 100 ppb Ag^+ (A) and 100 ppb Pb^{2+} (B) in acetate buffer, pH 5.2, with and without a N_2 purge. Image adapted from McGaw, et. al.[9]

In order to determine which of these possibilities was true, a series of experiments was performed to measure the residual Pb on the diamond electrode. In the case where PbO_2 is formed there would be Pb remaining on the surface after stripping, but in the case where Pb is chemically oxidized there would not. Powder X-ray diffraction (XRD) was used to determine the presence of the Pb. Initially, a spectrum was taken of the nanocrystalline diamond electrode to determine which peaks were due to the diamond (Figure 4.2), and a second spectrum was taken of the electrode after electrochemical deposition of Pb (Figure 4.2).

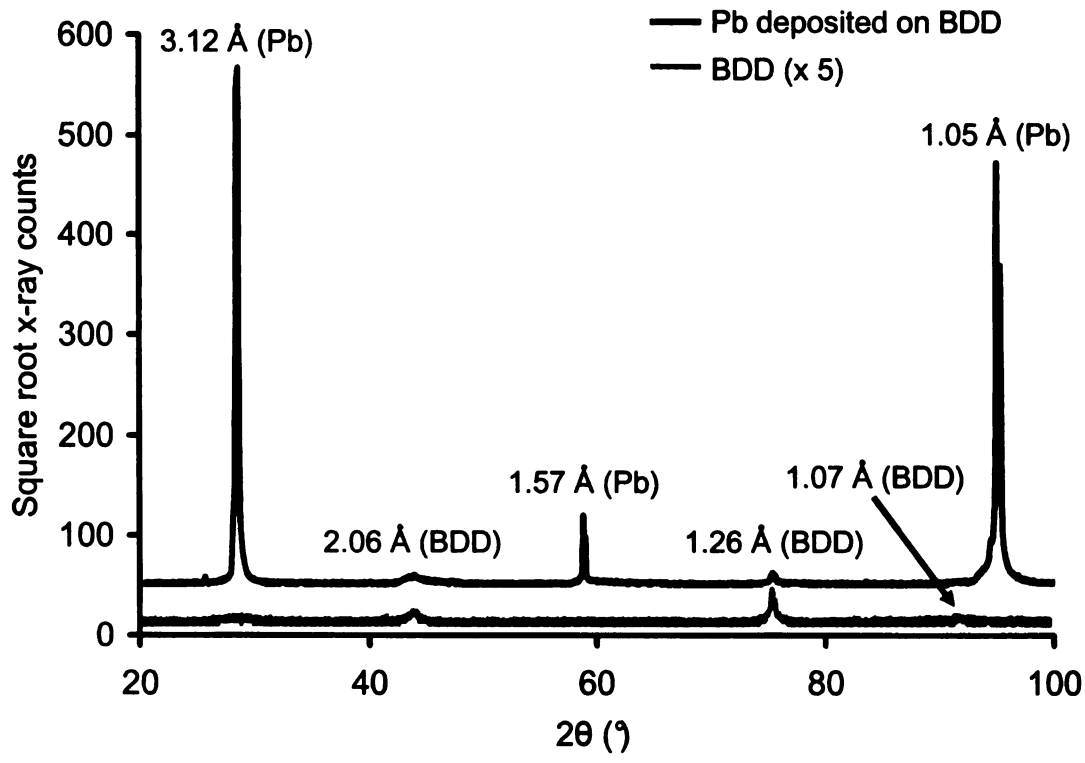

Figure 4.2. Powder XRD spectra taken of a bare diamond electrode (gray) and a diamond electrode with Pb electrochemically deposited on the surface (black). Peaks due to the diamond are marked with BDD and peaks due to Pb are also marked accordingly. The BDD signal is multiplied by 5 and spectra are offset slightly for clarity.

There are three peaks from the diamond, 2.06 Å, 1.26 Å, and 1.07Å, which correspond to the 111, 220, and 311 crystal faces, respectively.[5] There are also three peaks that are due to the Pb. The lattice spacings were compared with lattice spacings of reference materials: Pb, $PbO_{1.44}$, and PbO_2, see Table 4.3.[10-12] The peaks obtained in the experimental sample (i.e., Pb on BDD) do not directly correspond with any of the reference materials; the closest correlation is with $PbO_{1.44}$. There are peaks that are missing (e.g., 2.6 – 2.8 Å range), and the intensity ratios do not match the reference material. Notice that the different lattice spacings correspond to different crystallographic orientations of the

material (e.g., 111). The reference spectra were taken of powdered materials where the sample in this case was deposited on a surface. When the Pb deposits on the surface certain orientations may be preferential which would explain why all of the peaks from the reference material are not present or are at different ratios in the experimental results. In summary, it appears the Pb deposited on the BDD surface is a mixture of Pb and PbO_2. The electrode was removed from the electrochemical cell after electrodeposition and the Pb deposits were exposed to air so it is likely that some amount of Pb oxidation occurred prior to XRD analysis.

Table 4.3. Powder X-ray diffraction data for reference materials for Pb, $PbO_{1.44}$, and PbO_2. d is the lattice spacing, intensity indicates the relative intensity of the peaks, and hkl is the crystallographic orientation. The entries that are bolded and italicized are closest to the peaks seen experimentally.

Pb[10]			**$PbO_{1.44}$**[12]			**PbO_2**[11]		
d (Å)	**Intensity**	**hkl**	**d (Å)**	**Intensity**	**hkl**	**d (Å)**	**Intensity**	**hkl**
2.86	100	111	***3.16***	***100***	***111***	***3.09***	***100***	***111***
2.48	50	200	2.73	80	200	2.67	80	200
1.75	31	220	1.93	65	220	1.89	80	220
1.49	32	311	1.65	70	311	1.61	80	311
1.14	10	331	***1.58***	***11***	***222***	***1.54***	***30***	***222***
			1.26	14	331	1.34	30	400
			1.22	17	420	1.23	60	331
			1.05	***11***	***511***	1.20	80	420
						1.09	60	422

Two more samples were then generated, first, was a diamond electrode that had Pb electrochemically deposited and stripped (ASV) in a solution that was purged with N_2, the second was created the same way but the solution was

not purged with N_2. These two samples were analyzed only in the regions where Pb or BDD peaks were expected. The results are displayed in Table 4.4.

Table 4.4. Comparison of X-ray counts for peaks from XRD spectra of four diamond electrodes, bare, with Pb, Pb stripped - N_2 purge, and Pb stripped - no N_2 purge. The - indicates no peak seen above the background. N/A indicates this region was not scanned

d (Å)	X-ray counts			
	Bare	With Pb	Pb stripped – N_2 purge	Pb stripped – no N_2 purge
3.12 (Pb)	20	262000	133	-
2.06 (BDD)	43	110	N/A	43
1.57 (Pb)	-	4940	-	N/A
1.26 (BDD)	130	170	N/A	N/A
1.07 (BDD)	12	-	N/A	13
1.05 (Pb)	-	179000	63	-

The electrode that was prepared by depositing and stripping the Pb in a N_2 purged solution showed a small amount of Pb. The peaks, corresponding to d-spacing of 3.12 and 1.05 Å, were less than 1% of the size of the peak when Pb was deposited on the diamond (see Table 4.4). While XRD is only semi-quantitative this still suggests that there is only a small amount of residual Pb. For the electrode prepared by depositing and stripping the Pb in a solution that was not N_2 purged all peaks due to Pb were below the limit of detection. BDD peaks were still visible on this electrode, and were comparable to the signal seen for the bare BDD, indicating that the instrument was functioning properly, and the sample was mounted correctly. Therefore, there was no Pb detected in the case where no N_2 purge was used. This suggests that the lower current observed

when no N_2 purge was used results from chemical removal (oxidation) of the Pb from the surface of the electrode prior to electrochemical stripping.

4.3. Development of a Sampling Procedure

As indicated above, to make the technique practical for on-board monitoring, several adjustments were necessary. First, a method for introducing the buffer, adjusting the pH, and possibly remediating the effect of the dissolved O_2 present. Also a cell needed to be designed for use in microgravity environments.

4.3.1. Addition of the Supporting Electrolyte

An acetate buffer concentrate was developed that could be used to adjust the solution pH and add supporting electrolyte to the water sample. The buffer concentrate consisted of a high concentration of acetate salt (8000 ppm) in a 5% acetic acid solution. The composition of the solution was determined semi-empirically. The goal was to add 100 µL buffer concentrate to a 5 mL water sample, since this would only cause a 2% change in overall volume. The Henderson-Hasselbalch equation was used to calculate the amount of acetate needed to create a solution of pH 5.2 with an overall electrolyte concentration of 0.1 M. The solution was prepared, and the amount added was adjusted experimentally until the proper pH was reached. The final amount was 147 µL added to a 5 mL sample.

The second solution issue to address was the effect of the dissolved O_2 on the stripping voltammetric current, particularly for Pb. While a linear calibration curve was observed for the detection of Pb^{2+} even without an N_2

purge, the minimum detectable concentration was 50 ppb (S/N ≥ 3). This concentration is too high to be useful to assess toxicity of potable waters, as the limit of detection needs to be at or below the EPA drinking water standard. An approach that was explored involved the addition of an oxygen scavenging molecule to the solution to chemically remove the O_2 before analysis. Ascorbic acid was selected because it is a good O_2 scavenger that has been used previously for anodic stripping analysis.[13] Also, it is a non-toxic molecule; in fact, it is a common health supplement. Therefore, its addition to the water supply should pose no health problems. Based on previous use of ascorbic acid for stripping voltammetry a concentration of 0.1 M was chosen.[13] The ascorbic acid was added to a solution containing 100 ppb Pb^{2+} in the standard acetate buffer solution (pH 5.2). Anodic stripping voltammetric *i-E* curves were recorded in this solution, both with and without a N_2 purge. These voltammetric *i-E* curves were then compared to ones recorded without ascorbic acid (Figure 4.3).

From the figure, it is easy to see that ascorbic acid does have a positive effect on the Pb stripping current when dissolved O_2 is present. However, the overall signal with an N_2 purge is not as high as the case where no ascorbic acid is added. While the cause of this is unknown, it is possible that the high concentration of ascorbic acid (0.1M) is affecting the deposition of the Pb^{2+} either by complexing the Pb^{2+} in the solution phase or by adsorbing to the deposited Pb and preventing further deposition at that site.

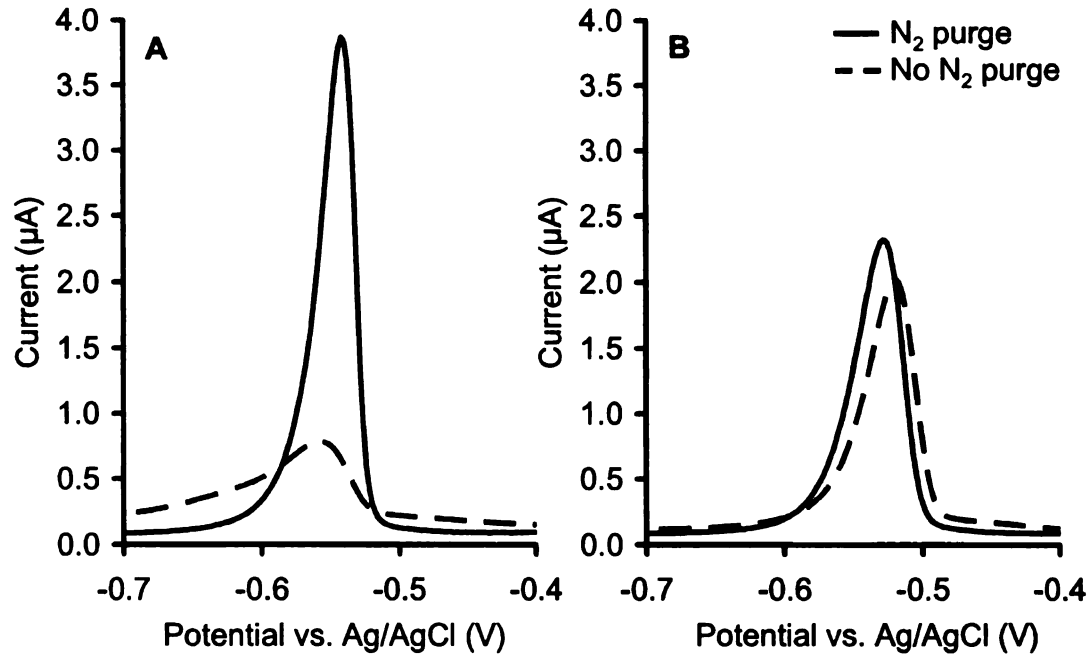

Figure 4.3. Anodic stripping voltammetric *i-E* curves for Pb were recorded in a solution containing, 100 ppb Pb^{2+} in acetate buffer, pH 5.2, with 30 ppm Ca^{2+} and 5 ppm Mg^{2+}. (A) no added ascorbic acid and (B) 0.1 M ascorbic acid.

4.3.2. Cell Design

An electrochemical cell was designed as a prototype for use in microgravity (Figure 4.4). When assembled, the cell was fully sealed, and had 3 luer ports with valves that served as inlets and outlets for the solution. The working electrode was secured between a viton o-ring and a copper cylinder for backside contact. A sleeve of Teflon was placed around the copper cylinder and was threaded to screw the assembly to the body of the cell. The reference electrode port was a swagelok fitting in the Plexiglas cover that was intended to be used with a "no-leak" Ag/AgCl reference electrode (EE-009, Cypress Systems, Inc., Lawrence, KS). The assembly was a cube with a side length of 46 mm; the inner chamber was also cubic with a side length of 18 mm. The inner

volume was 5 - 6 mL. The auxiliary electrode was a coil of Pt wire sealed in the Teflon side wall.

Three inlet and outlet ports were placed in the cell to enable easy loading, replacement, and rinsing of fluids. The luer fittings were used for ease of interfacing with NASA's current water system and sample bags. The cell could be used either with syringes to manually fill and empty the cell, or by connecting the system to a pump for automated flow.

Proper mixing of the water sample with the supporting electrolyte is a critical step with this cell. This was accomplished in the following manner. Two syringes were used; one contained 300 µL of buffer concentrate and the second contained 10 mL of water sample. The two syringes were connected using a male-to-male luer connection. The buffer concentrate was injected into the larger syringe containing the water sample, allowing the two solutions to mix. The syringe containing the combined solution was attached to an open inlet valve on the cell. A second valve was opened to allow the internal air to be displaced by the sample solution. The water solution was introduced into the cell slowly to minimize the entrapment of air. Once the cell was filled any remaining air was dislodged from the walls by tapping. The collected air was then displaced with additional sample introduction. Once the air was completely removed the values were closed, and the cell was ready for analysis.

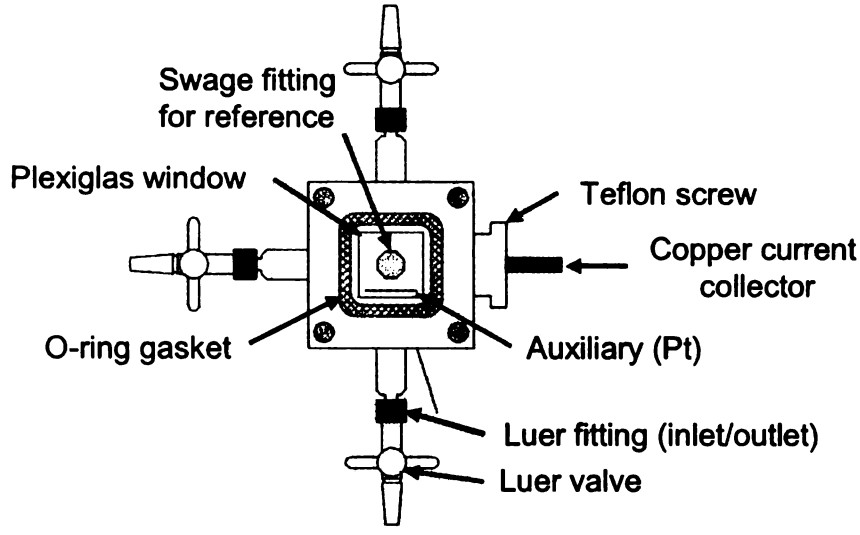

Top view

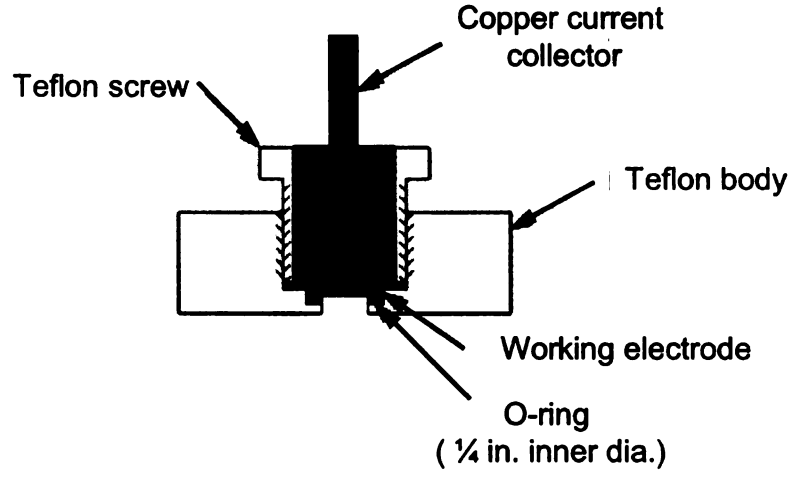

Cut away view of working electrode

Figure 4.4. A diagram of the sealed electrochemical cell designed for use in microgravity. The body is made of Teflon. Three luer fittings with valves serve as inlets and outlets. The planar working electrode is held in place by a copper cylinder inside a Teflon screw. The working electrode area is defined by a Viton o-ring (0.32 cm^2).

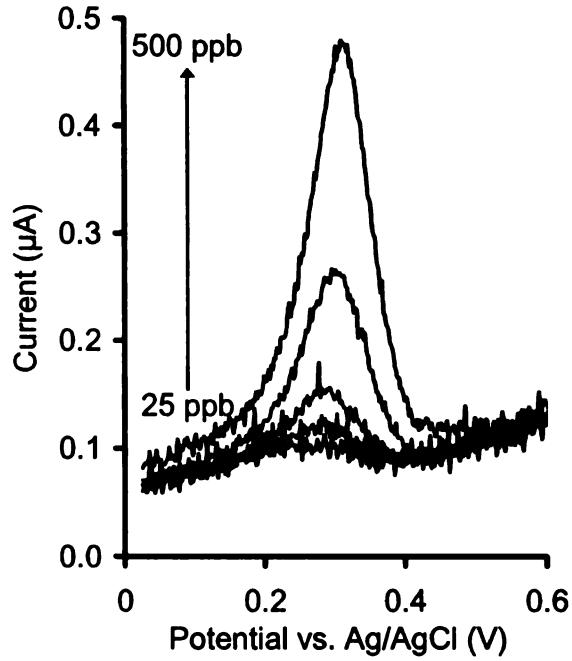

Figure 4.5. Anodic stripping voltammetric *i-E* curves for Ag in the microgravity prototype cell. Measurements were made using Ag^+ solutions ranging in concentration from 25 – 500 ppb. Buffer concentrate was used to add electrolyte, the concentration in the final solution was 0.1 M acetate, pH of 5.2. The deposition time was 3 min.

A calibration curve was constructed for Ag^+ using this procedure to determine the sensitivity of the method. The calibration curve was linear (r^2 > 0.99) for both current and charge (area) with sensitivities of 0.8 nA/ppb and 47 nC/ppb, respectively. The stripping voltammetric *i-E* curves used for the calibration curve are presented in Figure 4.5. In addition to the microgravity, cell a battery operated potentiostat (PG580, Princeton Applied Research, Oak Ridge, TN) was used to demonstrate the usefulness of the technique with equipment that could be used on space station. Because this is a smaller model and is battery operated it does not contain the filtering capability of a bench model

potentiostat, and this contributed to the noise seen in the voltammetric *i-E* curves.

4.4. Analysis of Simulated ISS Water

Simulated potable and technical water samples were provided by the Wyle Laboratory (Johnson Space Center) for analysis. The potable sample contained both Ag^+ and the Ca^{2+} and Mg^{2+} formate salts, and the technical sample contained just Ag^+. These simulants were evaluated using two cells: the traditional single compartment 3-electrode cell with the electrode mounted from the bottom and the microgravity prototype cell. Calibration curves were generated, using standard solutions of Ag^+, ranging in concentration from 350 to 550 ppb. All solutions were prepared using deionized water. The acetate buffer concentrate was used as the supporting electrolyte and for pH adjustment. In the open cell, the acetate buffer concentrate was added directly to the cell containing the water sample (147 µL concentrate per 5 mL water). The simulant samples were analyzed the same way as the calibration standards, and the concentrations were determined from the standard calibration curves. The results for each of the cells are displayed in Table 4.5.

Using both cell types, the Ag^+ concentration determined experimentally was close to the NASA specified concentration with an error of less than 5%. The exception to this is the result for the technical water in the standard cell. These results demonstrate two things. First the ASV method using a buffer concentrate provides accurate values for the Ag^+ concentration. Second, the microgravity cell functions well for this measurement. The standard deviation for

the concentrations obtained with the microgravity cell are a bit larger, however, the portable potentiostat was used with this cell, and the slightly higher background noise of this instrument and could have contributed to the larger standard deviations.

Table 4.5. Results from the analysis of Ag^+ in NASA simulated potable and technical water samples. Each water sample was measured in both the open cell as well as the microgravity cell. The error is the standard deviation of concentration calculated by 3 runs. The % error is calculated with respect to the specified value by NASA, which was determined by ICP-MS.

NASA (ICP-MS) (ppb)	Open Cell (ppb)	% Error	Microgravity Cell (ppb)	% Error
Simulated Potable Water				
422	432 ± 4	2 %	432 ± 13	2%
Simulated Technical Water				
480	530 ± 5	10%	506 ± 15	5%

4.5. Long-Term Response Stability

The last performance criterion evaluated was the long-term stability of the electrode response. Since replenishing missions are months apart, it is important that the electrode maintain a steady signal over this time period. To evaluate this, a standard water sample containing 400 ppb Ag^+ was prepared in deionized water, and analyzed three times per week. A single electrode was used for all tests, and the electrode remained mounted in the electrochemical cell during this period to ensure that the same area was used in each measurement. The cell used was a plastic version of the open cell made of high density polyethylene (HDPE). The water sample (5 mL) was added to the cell and mixed with a small amount (147 µL) of acetate buffer concentrate (which also contained Ca^{2+} and Mg^{2+} salts). At the end of each run a cleaning step was performed,

holding the electrode at a potential of 0.6 V with convection (N_2 bubbling) for 5 min to ensure a clean surface for the subsequent analyses. The electrode was stored in one of two ways, wet or dry. For the wet storage, deionized water was added to the cell at the end of the analysis. Dry storage involved removing all of the liquid from the cell and storing the electrode exposed to the atmosphere. The results from each of these stability tests are shown in Figures 4.6 and 4.7.

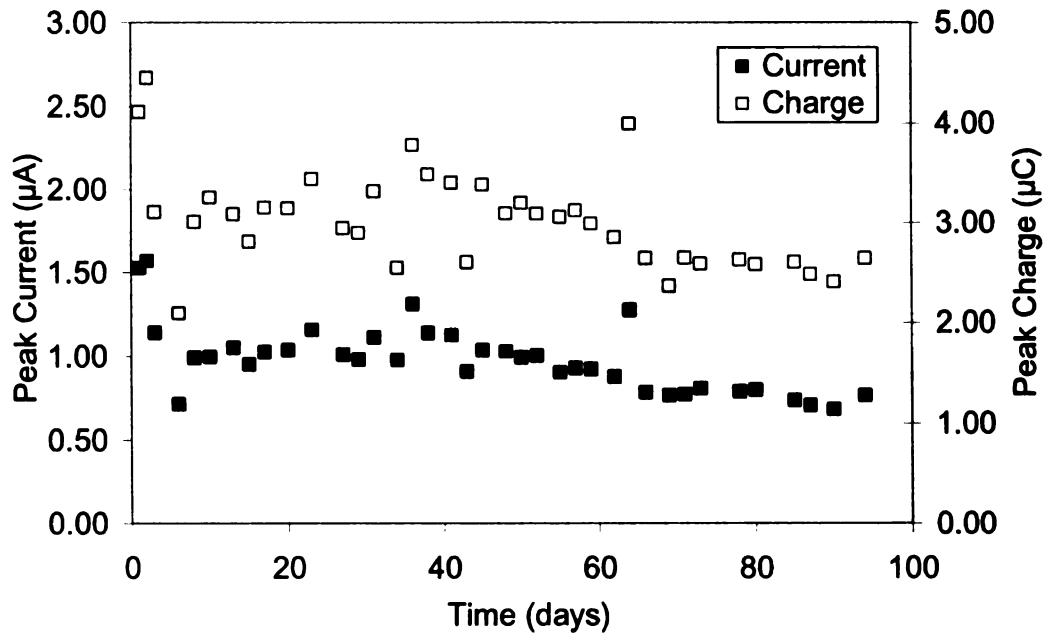

Figure 4.6. Stability test of a 400 ppb Ag^+ solution using a single diamond electrode. The electrode was stored wet, under deionized water, between measurements.

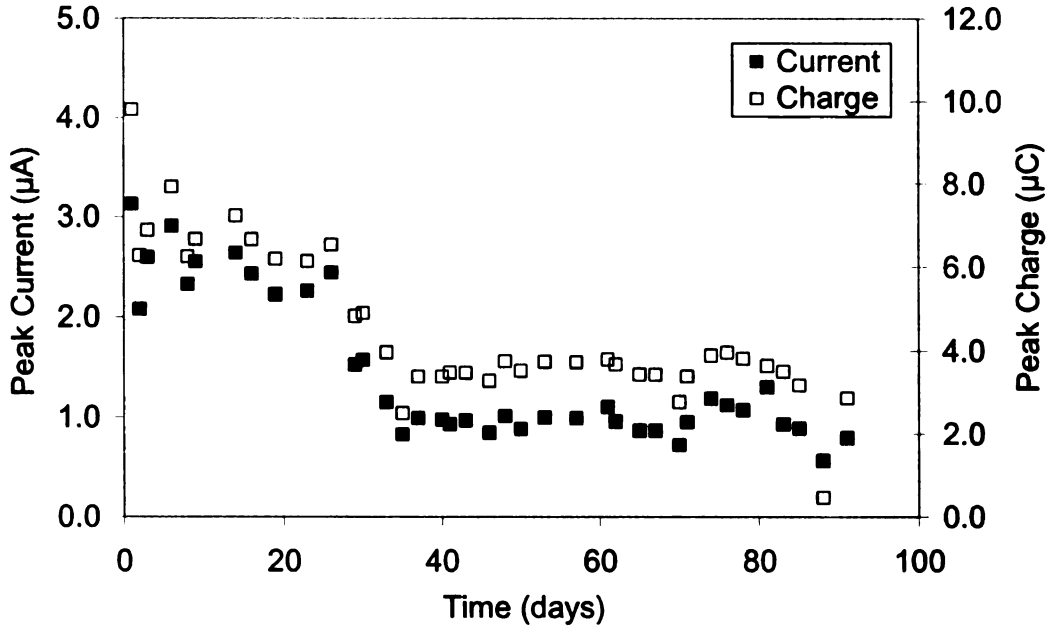

Figure 4.7. Stability test of a 400 ppb Ag^+ solution using a single diamond electrode. The electrode stored dry between measurements.

In the wet storage stability test (Figure 4.6) the response was very stable over the entire 90 day period with relative standard deviations of 9.3% and 9.1% for peak current and charge respectively. The dry storage had some fluctuations in the data in the initial 35 days; however, once the response stabilized the relative standard deviations were comparable to what was obtained with the wet storage method: 11.7% and 10.4% for peak current and charge respectively. Both the wet and dry storage had the same average value for peak current (1 µA) and peak charge (3 µC). It appears that the wet storage is a better method because it avoids the initial stabilization time, and the relative standard deviations are a little lower.

4.6. Conclusions

A ground-based ASV method was modified for possible on-orbit use. In general, BDD working electrodes provide low detection limits, excellent response precision, and good response stability for several priority metal ions, including Ag^+. The ability of the method to provide quantitative information on the Ag^+, Cu^{2+}, Pb^{2+}, and Cd^{2+} levels in water was not compromised by increasing the supporting electrolyte pH, mineralizing the water with Ca^{2+} and Mg^{2+} salts, or eliminating the N_2 purge step to remove dissolved O_2. The exceptions for the effect of dissolved O_2 were Pb^{2+}, and Cu^{2+}, however, the use of ascorbic acid offered a promising mitigation to this problem. The electrode exhibited good long-term response stability, observed for Ag^+ (<10% relative standard deviation in response over 90 days). Importantly, preliminary measurements of simulated transfer water samples revealed that the diamond thin-film electrode provides an accurate measurement of Ag^+ in the microgravity prototype cell.

4.7. References

(1) Plumlee, D. K.; Mudgett, P. D.; Schultz, J. R. *SAE Technical Paper 2002-01-2537 32nd International Conference on Environmental Systems* **2002**.

(2) Mudgett, P. D.; Benoit, M. J.; Schultz, J. R. *SAE Technical Paper 2002-01-2532 32nd International Conference on Environmental Systems* **2002**.

(3) Plumlee, D. K.; Mudgett, P. D.; Schultz, J. R. *SAE Technical Paper 2003-01-2401 33rd International Conference on Environmental Systems* **2003**.

(4) Swain, G. M. In *Electroanal. Chem.*; Bard, A. J., Rubinstein, I., Eds.; Marcel Dekker, Inc., 2004; Vol. 22, pp 181-277.

(5) Show, Y.; Witek, M. A.; Sonthalia, P.; Swain, G. M. *Chem. Mater.* **2003**, *15*, 879.

(6) Sonthalia, P.; McGaw, E.; Swain, G. M. *Anal. Chim. Acta* **2004**, *522*, 35-44.

(7) Wang, J. *Stripping Analysis Principals, Instrumentation, and Applications*; VCH Publishers: Deerfield Beach, Florida, 1985.

(8) Lund, W.; Onshus, D. *Anal. Chim. Acta* **1976**, *86*, 109-122.

(9) McGaw, E.; Sonthalia, P.; Swain, G. M. *SAE Technical Paper 2005-01-2888 35th International Conference on Environmental Systems* **2005**.

(10) In *Powder Diffraction File*; McClune, W. F., Ed.; International Centre for Diffraction Data: Swarthmore, PA, 1986, pp 4-686.

(11) In *Powder Diffraction File*; McClune, W. F., Ed.; International Centre for Diffraction Data: Swarthmore, PA, 1986, pp 22-389.

(12) In *Powder Diffraction File*; McClune, W. F., Ed.; International Centre for Diffraction Data: Swarthmore, PA, 1986, pp 27-1201.

(13) Florence, T. M.; Farrar, Y. J. *Electroanalytical Chemistry and Interfacial Electrochemistry* **1973**, *41*, 127-133.

CHAPTER 5

ANALYSIS OF HEAVY METAL IONS IN URINE

5.1. Introduction

Analysis of heavy metals in biological fluids can be an important tool for diagnostics as well as monitoring of occupational exposure. High levels of toxic metals in humans can indicate a single or a prolonged exposure, and it is important that there are clinical tools for the analysis of these analytes in humans. Depending on the properties and interactions of the metal ions in the body, they will be excreted in different ways, and will be present at different concentrations in different body fluids. For example, Cd^{2+} is more likely to appear in the urine, while Pb^{2+} is more likely to appear in the blood.[1] There are also essential metals (Zn^{2+}, Cu^{2+}) that can be found in the urine.[1] It is important to monitor these metals as well, since increased or decreased levels can indicate a problem. For instance, elevated Cu^{2+} levels in the urine can be an indicator of Wilson's disease.

Anodic stripping voltammetry is a common method for determination of metal ion concentration. Traditionally this type of analysis has been done using a Hg based electrode (e.g., hanging drop, thin-film); however, there have been recent attempts to replace the Hg based electrodes with a more environmentally friendly electrode material. Boron-doped diamond (BDD) is a relatively new electrode material that is being developed for stripping analysis by many groups. As discussed in Chapter 3, BDD is comparable to a more traditional Hg-coated glassy carbon electrode in a simple aqueous media.[2]

Atomic adsorption spectroscopy[3-5] and anodic stripping voltammetry (ASV) are commonly used methods for analysis of urine samples. For ASV it is typical that a digestion step is used because of the soluble proteins present in the urine. Many digestion procedures, including hot acid,[6-9] acid and ultrafiltration,[10] microwave digestion,[11-13] acid digestion bombs,[14, 15] dry ashing,[16] and freeze drying,[17] have been used successfully. Some have even used a polymer coating on the electrode to prevent interferences from compounds in the urine.[18, 19] Direct determination of metal ion concentration in urine has been done using both Hg-based electrodes[20-22] and glassy carbon electrodes.[23]

In this study, rat urine and urine simulant were analyzed by ASV without digestion or acidification. There were several factors in this decision: ease of analysis, the naturally high electrolyte concentration of the urine, and the fouling-resistant properties of the BDD, which make it a suitable candidate for the direct analysis of the urine. Also in preliminary studies the urine was acidified, however, this resulted in an interfering peak in the potential range of Cd oxidation. The identity of this peak is not known, however, it is has also been observed by Pauliukaite and co-workers.[9]

Cd^{2+} was the metal ion chosen as the focus of this study because the urine concentration of Cd^{2+} is the most important clinical indicator of excessive cadmium exposure, whereas other metals are typically analyzed in the blood (e.g., Pb^{2+}).[1]

5.2. Deposition Parameters

Toxic levels of Cd^{2+} in urine are in the low ppb to high ppt range. For example a study by Yassin and Martonik reported levels ranging from 0.01 ppb (normal) to 15.57 ppb (toxic).[5] Therefore, low detection limits are necessary for this analysis. The ASV detection limit of Cd^{2+} in an acetate buffer solution with a 210 s deposition was found to be 1.0 ppb using BDD as a working electrode (see Chapter 3). A lower detection limit was desired for this analysis; to lower the detection limit the deposition parameters (e.g., deposition time and ion flux) were studied.

Initially, a single solution of 250 ppb Cd^{2+} in simulated urine (pH 8.8) was used, and the deposition time was varied between 2 and 360 seconds (no convection). The results of this study are shown in Figure 5.1 A. The points are an average of 3 measurements and the error (standard deviation) is within the size of the markers.

It is clear that increasing the deposition time caused the peak current to increase, up to a point. However, the current begins to level off around 200 s with little enhancement occurring with additional time. The deposition conditions used in previous studies were 180-210 s, and increasing the deposition time beyond this does not appear to have a significant benefit.

The curve (Figure 5.1 A) begins to level off because the mass transport of the Cd^{2+} to the electrode surface is limited. By adding convection during deposition the flux of Cd^{2+} to the electrode will be enhanced to give higher stripping peak currents. Several methods of convection were explored: stirring

with a stir bar, stirring with a rotator with a variety of "fins" attached, and bubbling with N_2 gas. The N_2 gas was the most successful method yielding the largest enhancement of peak current. To regulate the N_2 flow, a gas flow meter was used to ensure the same flow rate was used each day. In addition the tubing that was used was marked to ensure that the gas line was placed at the same height with respect to the electrode.

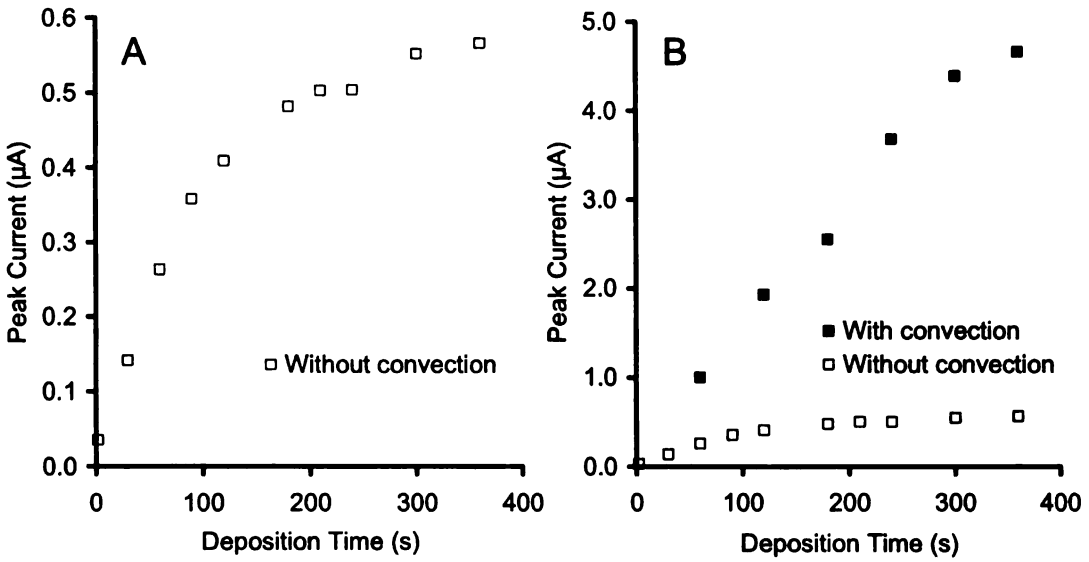

Figure 5.1. Peak current as a function of deposition time for 250 ppb Cd^{2+} in urine simulant (pH 8.8). Deposition time varied between 2 s and 5 minutes. A) no convection method used, B) N_2 bubbling used for convection. Each point is an average of 3 measurements.

Using N_2 as a convection method the deposition time was again varied (Figure 5.1 B). The first observation is that the current is much higher than the case without convection (plotted on same the graph for comparison). For example, at 60 s the peak current was 0.26 µA without convection versus 1.0 µA with convection. Based on these experiments, a deposition time of 300 s (with convection) was selected for use in analysis.

5.3. Detection Figures of Merit

To characterize the BDD electrode for use directly in a urine sample, the detection figures of merit in the urine simulant were determined. A calibration curve was generated for concentrations in the 10 to 250 ppb range (Figure 5.2). The calibration curve is linear ($r^2 > 0.99$) for both peak current and peak charge (area) with sensitivities of 27.3 nA/ppb and 99.7 nC/ppb, respectively. As expected the sensitivity in the urine simulant is higher than the sensitivity reported in standard acetate buffer at pH 5.2 (14.7 nA/ppb) due to the longer deposition time and added convection.[2] The linear dynamic range was not specifically investigated, however, linearity in the response was observed over 2 orders of magnitude in the range tested (10 – 250 ppb).

The lowest concentration of Cd^{2+} detected in the urine simulant with a signal/noise (S/N) > 3 was 10 ppb (S/N=5). This is higher than the 1.0 ppb reported for the standard solutions in acetate buffer pH 5.2.[2] While the sensitivity of this measurement is higher than in the acetate buffer, the noise is also larger in the urine simulant, 6 nA vs. 2 nA. The limit of detection is a function of both the noise as well as the sensitivity. During the stripping step in the urine simulant, the N_2 was still bubbling and this added to the background noise. The noise could be lowered by removing the N_2 line before the stripping step but because this gas line was place in the cell manually it was difficult to reproducibly remove it just prior to the stripping step. Since the convection from the bubbling enhances the deposition, if it was not moved at exactly the same time it lead to problems with the reproducibility of the stripping curves. Therefore, it was

decided that the increased noise level was more tolerable than the poor reproducibility. However, if an automated convection method was used it could be reproducibly shut off before stripping, and it is expected that the noise would decrease also leading to a decrease in the limit of detection.

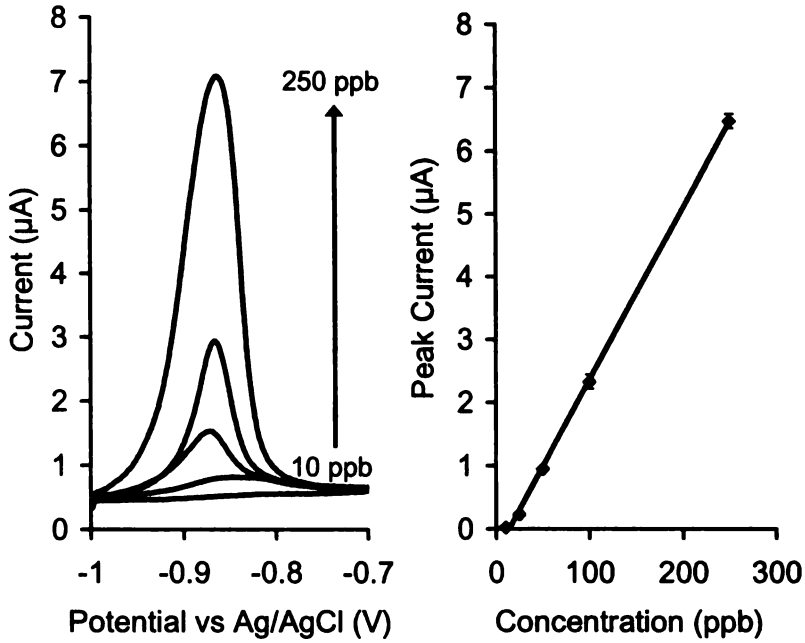

Figure 5.2. Anodic stripping curves (left) and calibration curve (right) for urine simulant (pH 8.8) with Cd^{2+} concentrations in the range of 10 to 250 ppb. Deposition occurred at -1.0 V vs. Ag/AgCl for 300s with convection (N_2 bubbling) Error bars on calibration curve represent standard deviation.

For the method to be useful, it is important to have run-to-run reproducibility as well as electrode-to-electrode reproducibility. This was tested on 3 nanocrystalline diamond electrodes, 3 runs each, using 75 ppb Cd^{2+} in the urine simulant. The average peak currents and standard deviations are shown in Table 5.1 for each of the electrodes as well as overall. The run-to-run variability is described by the relative standard deviation for each electrode, and is less

than 5% for each. The electrode-to-electrode variability is also excellent at only 6%.

Table 5.1. Reproducibility of Cd^{2+} signal on 3 BDD electrodes. 75 ppb Cd^{2+} in simulated urine (pH 8.8).

	Average Peak Current (μA)	**Relative Standard Deviation**
Electrode 1 (n=3)	1.08 ± 0.03	2.72%
Electrode 2 (n=3)	0.95 ± 0.01	0.65%
Electrode 3 (n=3)	1.01 ± 0.05	4.44%
3 Electrode Average (n=9)	**1.01 ± 0.06**	**6.15%**

5.4. Standard Addition

Real urine samples posses a complex matrix and variable pH so the Cd^{2+} concentrations are best determined by the standard addition method. For the standard addition, 10 ppb Cd^{2+} in urine simulant was used as the initial solution, and two additions to create 20 and 30 ppb Cd^{2+} were made for each sample. A solution with a high concentration of Cd^{2+} was added to cause a minimal change in overall volume. The change in volume was accounted for in plotting the added Cd^{2+} concentration. The concentration of the initial urine (10 ppb Cd^{2+}) was determined by this procedure to be 1.7 ppb, an error of 83%. One possible source for this error is the complexation of Cd^{2+} by other constituents in the sample that would reduce its activity.

5.5. Cadmium Complexation

If components of the urine simulant complex with the Cd^{2+}, then the stripping voltammetric current will be lower due to less free Cd^{2+} available for deposition. ASV will only yield a response, at the thermodynamic potential, for

free metal ions or metal ions in labile complexes.[24, 25] Components of the urine simulant that were tested as possible interferants were lactic acid, citric acid, and ammonia.

Calculations were performed initially using known formation constants to determine the amount of free Cd^{2+} available when each complexing agent is present at the concentration used in the urine simulant. To simplify the math, each component was considered individually. The formation constants used were obtained from Lange's Handbook and are shown in Table 5.2.[26]

Table 5.2. Formation constants for Cd^{2+} complexes.[26] Listed as cumulative formation constants where K_n is equal to $k_1k_2....k_n$ if k is the stepwise formation constants.

	log K_1	log K_2	log K_3	log K_4	log K_5	log K_6
Ammonia	2.65	4.75	6.19	7.12	6.80	5.14
Citric Acid	11.3	-	-	-	-	-
Lactic Acid	1.7	-	-	-	-	-

The estimated free Cd^{2+} concentration was calculated for several Cd^{2+} solutions ranging from 25 to 100 ppb Cd^{2+}, and the results are displayed in Table 5.3 as the percentage of the total Cd^{2+} dissolved in the solution that is free Cd^{2+}. It is clear that both the ammonia and citric acid have a major impact on decreasing the amount of free Cd^{2+} in solution.

These calculations were followed up by additional experiments that tested the effect of each complexing agent separately in an acetate solution at pH 8.8; the same pH as the urine simulant. Each solution contained 30 ppb Cd^{2+}. The resulting voltammetric *i-E* curves are displayed in Figure 5.3. The data show there is a significant effect from each of the complexing agents, with all three

causing a decrease in the peak current and charge as compared to the control. Ammonia and citric acid caused the stripping peak to shift slightly negative. The relative effect (ammonia > citric acid > lactic acid) is the same trend suggested by the calculations (Table 5.3).

Table 5.3. Calculated concentration of free Cd^{2+} in the presence of complexing agents: ammonia, citric acid, and lactic acid.

Ammonia (0.1 M)		
$[Cd]_{total}$(ppb)	$[Cd^{2+}]_{free}$ (ppb)	$[Cd^{2+}]_{free}/[Cd]_{total}$
25	0.02	0.07%
50	0.04	0.07%
75	0.06	0.07%
100	0.07	0.07%
Citric Acid (3 mM)		
$[Cd]_{total}$(ppb)	$[Cd^{2+}]_{free}$ (ppb)	$[Cd^{2+}]_{free}/[Cd]_{total}$
25	0.24	0.95%
50	0.48	0.95%
75	0.71	0.95%
100	0.95	0.95%
Lactic Acid (4 mM)		
$[Cd]_{total}$(ppb)	$[Cd^{2+}]_{free}$ (ppb)	$[Cd^{2+}]_{free}/[Cd]_{total}$
25	20.8	83.3%
50	41.7	83.3%
75	62.5	83.3%
100	83.3	83.3%

The effect of increasing the pH (8.8 in urine simulant compared to 4-5 in acetate buffer) was also considered as a cause for the inaccurate determination of Cd^{2+} concentration in the urine simulant. However, based on the Pourbaix diagram, increasing the pH from 4 to 9 at the deposition potential of -1.0 V vs. Ag/AgCl, has no effect on the Cd^{2+} concentration (i.e., $Cd(OH)_2$ formation).[27] This was confirmed by making anodic stripping voltammetric measurements in acetate buffer solutions ranging from pH 5 to 9. There was no change in the Cd^{2+} stripping peak potential, current, or charge.

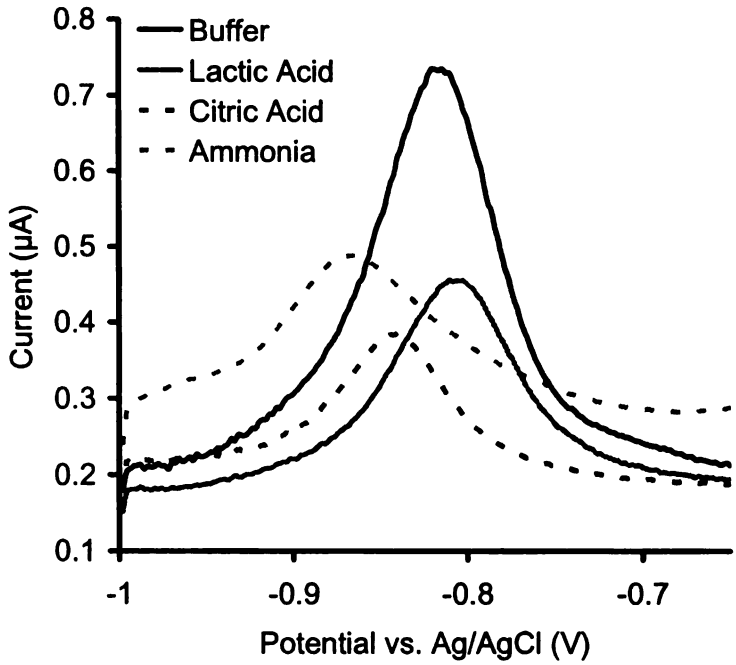

Figure 5.3. Anodic stripping voltammetric *i-E* curves for Cd in an acetate buffer, pH 8.8, containing 0.1M ammonia, 3mM citric acid, or 4mM lactic acid. 30 ppb Cd^{2+} deposited for 180 s with convection (N_2 bubbling).

Because complexation causes such a major decrease in the Cd stripping response, it is necessary to remove these interferences before analysis. This can be accomplished with a digestion. Several methods have been successfully used including hot acid,[6-9] acid and ultrafiltration,[10] microwave digestion,[11-13] or acid digestion bombs,[14, 15] as mentioned previously. Even though the BDD electrode may not be specifically affected by these components, they affect the electrochemical signal for Cd^{2+}.

5.6. Real Sample Analysis

To test the utility of the method on a real sample, rat urine was obtained for testing. The filtered (PTFE syringe filter, 0.1 μm) rat urine was directly analyzed with the diamond electrode. This curve is shown in Figure 5.4. No Cd stripping response was observed in the urine alone. Measurements were then made on urine samples spiked with higher concentrations of Cd^{2+}. Curves for concentrations between 90 and 300 ppb are also shown in Figure 5.4. Around a potential of -0.8 V an increase in current is seen indicating that the electrode is responding to the increasing Cd^{2+} concentration. The sensitivity of the measurement is poor as only a small response is seen at a high concentration of 300 ppb.

Because the rat urine contains other components (e.g., proteins) that are not present in the urine simulant, it was also important to evaluate the stability of the electrode response to check for any fouling effects. To accomplish this rat urine containing 300 ppb Cd^{2+} was added to the cell and several sequential runs were performed over a 6 hour time period (Figure 5.5).

There was no evidence of any electrode fouling over the course of the measurements. After the initial 20 measurements the response stabilized, and the relative standard deviation (RSDs) for runs 20 – 35 was 3.1% for current and 3.2% for area. These values indicate that the diamond electrode is very stable even in a complex matrix.

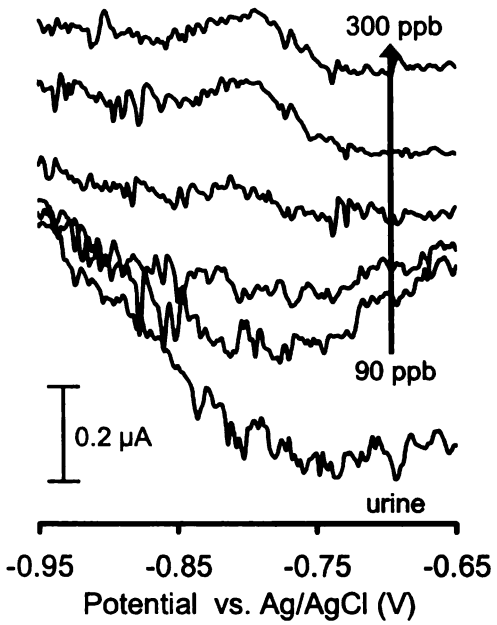

Figure 5.4. Anodic stripping voltammetric *i-E* curves in rat urine. Bottom curve is rat urine alone and aliquots of Cd^{2+} were added to increase the Cd^{2+} concentration to the range of 90 -300 ppb. Curves are offset for clarity.

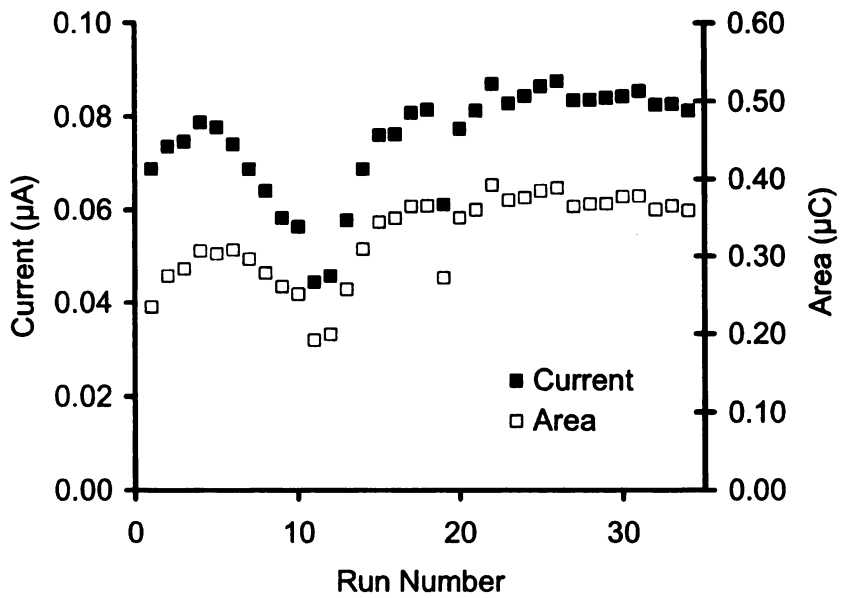

Figure 5.5. Stability test performed in 300 ppb Cd^{2+} in real rat urine. Measurements are sequential runs taken over a time period of approximately 6 hours. Deposition conditions, 300 s with convection (N_2 bubbling).

5.7. Conclusions

The Cd stripping signal can be enhanced by increasing the deposition time as well as adding a convection step to enhance the Cd^{2+} flux to the surface. The best deposition time was determined to be a 300 s with N_2 bubbling for convection. In the urine simulant a linear calibration curve was obtained over a range of 2 orders of magnitude (10–250 ppb), and the response was reproducible electrode-to-electrode (RSD 6%). A digestions step, or other purification step, to remove complexing agents, is imperative to obtain accurate Cd^{2+} concentrations. For the urine simulant, it was found that at least three components, ammonia, citric acid, and lactic acid, have a negative effect on the electrochemical signal by reducing the Cd^{2+} activity. This causes a higher limit of detection and inaccurate determination of the Cd^{2+} concentration by standard addition. A possible solution to this would be to digest the urine simulant prior to analysis, either using a hot acid digest or a microwave digest. The digestion would destroy the organic and inorganic molecules that were complexing the Cd^{2+} and lead to a more accurate determination of Cd^{2+}.

The diamond electrode performed adequately in a rat urine sample. An increased signal was observed for increasing concentrations of Cd^{2+}. The electrode showed no fouling effects from proteins or biological molecules in the real sample over a 6 hour period. Attempts were also made to determine the Cd^{2+} concentration in rat urine after centrifugation and filtration. Even though the electrode response was stable and reproducible, minimal sensitivity was observed for the metal ion.

5.8. References

(1) Goyer, R. A. In *Casarett & Doull's Toxicology: The Basic Science of Poisons,* 5th ed.; Klaassen, C. D., Ed.; McGraw-Hill: New York, 1996, pp 691-736.

(2) McGaw, E.; Swain, G. M. *Anal. Chim. Acta* **2006**, *575*, 180-189.

(3) Sharma, R. P.; McKenzie, J. M.; T., K. *J. Anal. Tox.* **1982**, *6*, 135-138.

(4) Castro Maciel, C. J.; Miranda, G. M.; Oliveria, D. P.; Siqueria, M. E. P. B.; Silveria, J. N.; Leite, E. M. A.; Silva, J. B. B. *Anal. Chim. Acta* **2003**, *491*, 231-237.

(5) Yassin, A. S.; Martonik, J. F. *J. Occup. Environ. Hyg.* **2004**, *1*, 324-333.

(6) Searle, B.; Chan, W.; Davidow, B. *Clin. Chem.* **1973**, *19*, 76-80.

(7) Lund, W.; Eriksen, R. *Anal. Chim. Acta* **1979**, *107*, 37-46.

(8) Jeong, E.-D.; Won, M.-S.; Shim, Y.-B. *Electroanal.* **1994**, *6*, 887-893.

(9) Pauliukaite, R.; Metelka, R.; Svancara, I.; Krolicka, A.; Bobrowski, A.; Vytras, K.; Norkus, E.; Kalcher, K. *Anal. Bioanal. Chem.* **2002**, *374*, 115-1158.

(10) Yantasee, W.; Timchalk, C.; Lin, Y. *Anal. Bioanal. Chem.* **2007**, *387*, 335-341.

(11) Pan, T. C.; Horng, C.-J.; Lin, S. R.; Lin, T. H.; Huang, C. W. *Biol. Trace Elem. Res.* **1993**, *38*, 233-241.

(12) Horng, C.-J. *Analyst* **1996**, *121*, 1511-1514.

(13) Horng, C.-J.; Horng, P.-H.; Hsu, J. W.; Tsai, J.-L. *Archives of Environmental Health* **2003**, *58*, 104-110.

(14) Kinard, J. T. *Anal. Lett.* **1977**, *10*, 1147-1161.

(15) Onar, A. N.; Temizer, A. *Analyst* **1987**, *112*, 227-229.

(16) Newberry, C. L.; Christian, G. D. *J. Electroanal. Chem.* **1965**, *9*, 468-472.

(17) Golimowski, J.; Valenta, P.; Stoeppler, M.; Nurnberg, H. W. *Talanta* **1979**, *26*, 649-656.

(18) Hoyer, B.; Florence, T. M.; Batley, G. E. *Anal. Chem.* **1987**, *59*, 1608-1614.

(19) Kefala, G.; Economou, A.; Voulgaropoulos, A. *Analyst* **2004**, *129*, 1082-1090.

(20) Kemula, W.; Kublik, Z. *Nature (London)* **1961**, *189*, 57-58.

(21) Copeland, T. R.; Christie, J. H.; Osteryoung, R. A.; Skogerboe, R. K. *Anal. Chem.* **1973**, *45*, 2171-2174.

(22) Herbeuval, X.; Maso, J. L.; Baudot, P.; Hutin, M. F.; Burnel, D. *Pathol. Biol.* **1975**, 379-386.

(23) Ramadan, A. A.; Mandil, H.; Asaad, W. *Asian J. Chem.* **2006**, *18*, 50-56.

(24) Vydra, F.; Stulik, K.; Julakova, E. *Electrochemical Stripping Analysis*; Ellis Horwood Limited: Chichester, 1976.

(25) Wang, J. *Stripping Analysis Principals, Instrumentation, and Applications*; VCH Publishers: Deerfield Beach, Florida, 1985.

(26) Dean, J. A., Ed. *Lange's Handbook of Chemistry*, 15th ed.; McGraw-Hill, 1999.

(27) Deltombe, E.; Pourbaix, M.; Zoubov, N. In *Atlas of Electrochemical Equilibria*; Pourbaix, M., Ed.; Pergamon Press Ltd.: Oxford, 1966, pp 414-420.

CHAPTER 6

ANALYSIS OF HEAVY METAL IONS IN BLOOD

6.1. Introduction

The analysis of biological fluids for heavy metals is important for clinical diagnosis and treatment of poisoning. As stated previously, in the discussion of analysis in urine, different metals will be present in different body fluids depending on the physiological activity of each. One metal ion that is important clinically, and that is found in the blood is Pb^{2+}. The Pb^{2+} is biologically similar to Ca^{2+}, and can replace Ca^{2+}, or possibly Zn^{2+}, thus affecting synaptic neuro-transmission.[1] Pb^{2+} can also replace Ca^{2+} in the bone, weakening it, and the half life of Pb^{2+} in the bone is 20 years.[1] The adverse health effects from Pb^{2+} are mainly neurological and hematological, but it can also affect reproduction. The Pb^{2+} concentrations at which some of these adverse health effects manifest themselves are displayed in Table 6.1.

Table 6.1. Minimum concentration of Pb^{2+} in blood when different health effects are observed.[1]

Effect	Pb^{2+} Concentration in Blood (ppb)	
	Children	Adults
Low IQ	100 – 150	
Hearing loss	200	
Encephalopathy	800 – 1000	1000 – 1200
Nephropathy	400	
Reproductive (e.g., sterility)		400
Anemia	800 – 1000	800 – 1000

Elevated Pb^{+} levels are particularly dangerous for children because they are growing and developing. According to the Centers for Disease Control and

Prevention (CDC), over 300,000 children in the United States have elevated blood Pb^{2+} levels (> 100 ppb).[2] They are committed to eliminating elevated blood Pb^{2+} levels in children by 2010. The CDC recommends that children at risk of high Pb^{2+} levels (e.g., live in a home with lead based paint) be tested yearly. Because of the large number of children who are tested, there is a need for a simple and quick measurement that could even be done in a doctor's office.

Graphite furnace atomic absorption spectroscopy is the most commonly used analytical technique for Pb^{2+} analysis in blood.[3] However, other methods may be better suited to high throughput analysis or screening in a doctor's office. Electrochemical methods are ideal for this type of analysis because they are portable, inexpensive, and easy to operate. Anodic stripping voltammetric analysis of Pb^{2+} in blood is becoming more routine, and there is even a commercial point-of-care testing system, LeadCare, developed by ESA, Inc. using this technique.[4-6]

A variety of working electrodes have been used for the analysis of Pb in blood including Hg,[7-9] Bi,[10, 11] and sp^2 carbon materials.[12] Boron-doped diamond (BDD) has many qualities that make it attractive for this type of analysis including resistance to fouling and a need for minimal activation pretreatment. The intent of this work was to examine the utility of BDD for blood analysis.

6.2. Sample Preparation

Anodic stripping voltammetry (ASV) is sensitive to the activity of free metal ions in solution. The metal ions must not be bound to other solution species, and must be able to be electrochemically reduced and deposited on the electrode

surface. More than 90% of the Pb^{2+} in blood exists in the red blood cells, and is associated with the cell membrane and the hemoglobin.[1] Therefore, a digestion method is routinely used to lyse the red blood cells, thereby releasing the Pb^{2+}. The ESA, Inc. procedure for this uses 0.3 M hydrochloric acid (HCl) mixed with blood in a 5-to-1 ratio. This mixed solution is then directly analyzed on their carbon electrode, and the HCl serves as the electrolyte for the electrochemical analysis. A similar preparation was used in these preliminary studies.

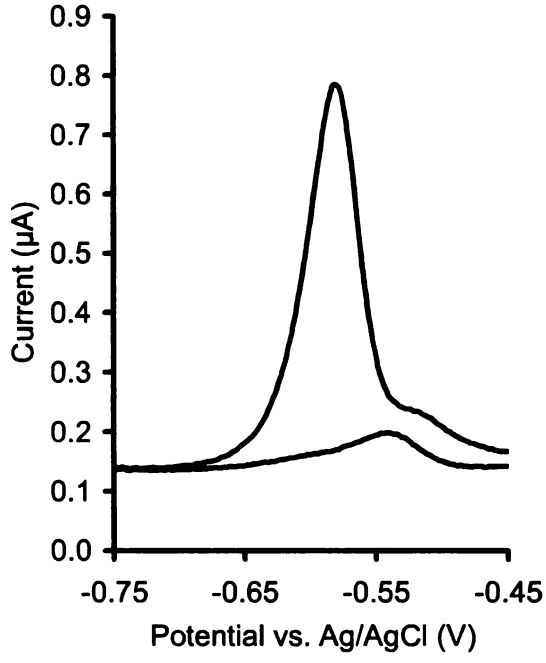

Figure 6.1. Anodic stripping voltammetric *i-E* curves for BDD in 0.1 M acetate buffer, pH 5.2, and 0.1 M NaCl, with 100 ppb Pb^{2+} (top) and without Pb^{2+} (bottom). The deposition time was 180 s.

In preliminary studies using HCl as an electrolyte, a second stripping peak, slightly more positive than the Pb peak, was observed. In acetate buffer alone the background is flat; no second peak is observed in the region of the Pb

peak. Therefore, it was supposed that the peak was related to the Cl^-. When Cl^- was added to the acetate buffer (0.3 M NaCl) the voltammetric *i-E* curve did have a second peak (Figure 6.1). For reference 100 ppb Pb^{2+} was added to the same buffer containing Cl^-, and the peak due to the Cl^- is observed adjacent to the Pb^{2+} peak. This is similar to what is observed when HCl is used as the electrolyte confirming that this peak is due to Cl^-.

6.3. Prevention of Fouling

Proteins adsorb on many surfaces; a process that can passivated an electrode making it unusable for measurement. Measurements in blood are challenging because of the large number of proteins present that can foul the electrode. Polar molecules weakly adsorb on BDD because of the relatively non-polar hydrogen surface termination and the absence of an extended π electron system.[13-16] BDD has been shown to have resistance to fouling from surfactants and proteins[17] making it potentially useful for analysis in whole blood. Even though the surface of BDD is typically resistant to fouling, preliminary analysis of Pb^{2+} in bovine blood (mixed 1 part blood to 5 parts 0.3 M HCl) yielded a small response that decreased with each subsequent run. The Pb stripping response could not be fully regained after exposure to the blood even after a 24 h soak in distilled water and an additional 20 min soak in isopropanol (Figure 6.2).

It was, therefore, necessary to develop a means to protect the electrode surface from molecular adsorption. There have been numerous polymeric coatings used for fouling prevention including dialysis membrane[18], polylysine/polystyrene,[19] cellulose acetate,[20-24] and Nafion.[7, 9, 25-33] Ultrasound

has been used to lesson the effects of fouling by acting to clean the surface in situ through cavitational activity of bubbles formed.[10] Nafion is a cation exchange ionomer that has been used as an electrode modification in numerous electroanalytical applications. It has been used with ASV for the determination of heavy metal ions in biological matrices.[7, 9, 25, 26] Because of the extensive literature based, Nafion was selected for use in this work.

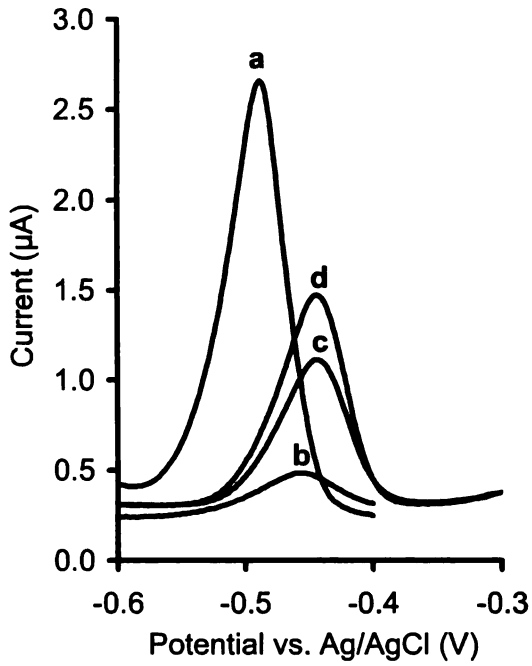

Figure 6.2. Anodic stripping voltammetric *i-E* curves of 450 ppb Pb^{2+} in HCl (1 part Pb^{2+} solution to 5 parts 0.3 M HCl), before exposure to bovine blood (a), immediately after exposure to bovine blood (b), after a 24 h soak in distilled water (c), and after an additional 20 min soak in isopropanol (d). The deposition time was 180 s.

6.3.1. Nafion Coating

There was no reported literature on Nafion-coated BDD electrodes, so the first task was to investigate the physicochemical properties of the film deposited on BDD. The electrode was modified with Nafion using a simple drop-coating

method. A 3% Nafion solution was prepared in ethanol, and 60 µL of this solution was dropped onto the BDD (~1 cm^2). This volume was sufficient to fully cover the surface. The solution was then allowed to dry for 20 min in a covered beaker to prevent contamination from particles in the air.[28] Care was taken to place the electrodes on a flat and level surface to ensure that the film dried uniformly.

The thickness of the Nafion film was estimated by weighing the electrode before and after coating. The Nafion weight (dry) was 0.0015 ± 0.0002 g. The density of hydrated Nafion is between 1.4 and 2.0 g/cm^3 (depending on the source of the Nafion and curing method).[34] Using this range of densities, knowing the film weight and area (1 cm^2), the film thickness was calculated to range from 7.7 to 11 µm. The uniformity of the film thickness was not specifically investigated; however, there were minimal refraction patterns on the surface. The absence of refraction patterns was consistent with a relatively uniform film thickness.

The negatively charged (highly acidic) sulfonate groups in the interior of the polymer electrostatically preconcentrate Pb^{2+} near the electrode surface. Because of this preconcentration the amount of metal phase formed during the deposition step is larger than that in the absence of the polymer. The increased metal phase loading leads to increased stripping signal (i.e., increased signal/background). The Pb stripping peak current in blood is plotted as a function of the preconcentration time for three different Pb^{2+} solution concentrations using a Nafion-coated BDD electrode (Figure 6.3).

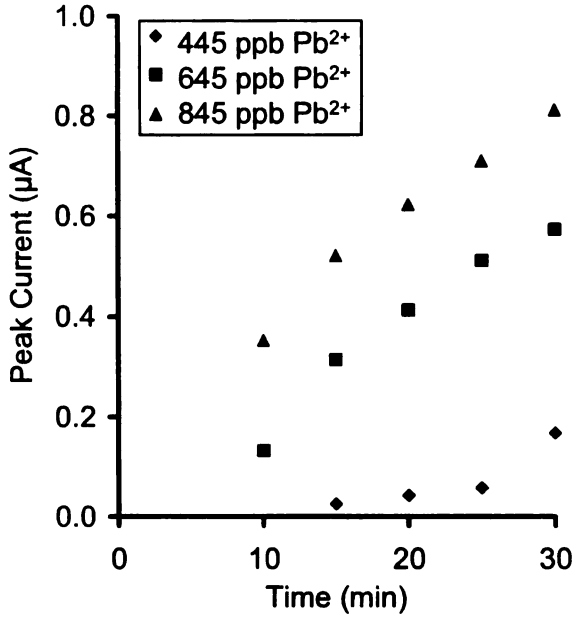

Figure 6.3. Pb stripping current for Pb^{2+} in bovine blood as a function of the preconcentration time. The blood was mixed 1:5 with 0.3 M HCl. The BDD electrode was coated with a Nafion film. The time axis indicates the amount of time blood solution was in contact with Nafion coated electrode before deposition began. The deposition time was 180 s.

The results reveal that longer preconcentration time, prior to deposition, for a given Pb^{2+} concentration, results in a larger stripping peak current. A single preconcentration time, the stripping current increased with the solution concentration. The peak current is influenced by the amount of Pb^{2+} preconcentrated in the Nafion film, which increases with time, until the polymer becomes saturated. The amount of Pb^{2+} loaded in the film depends on the flux of the Pb^{2+} into the polymer as well as the amount of time the polymer is in contact with the Pb^{2+} solution. Even though the time is increased the flux will decrease over time. The flux is related to electrostatic attraction and the concentration gradient, which will decrease as the concentration of Pb^{2+} increases. Therefore,

there is not a simple linear relationship between electrode exposure time and the amount of Pb^{2+} preconcentrated (i.e., electrochemical response).

It is also important that the Nafion film can be reproducibly deposited on the electrode surface. The drop-coating method was tested using three electrodes all cast and cured the same way. Each of these electrodes was then used to analyze for Pb^{2+} (445 ppb) in bovine blood. The resulting stripping peak currents and charges (areas) are presented in Table 6.2. The relative standard deviation (RSD) of the response is quite high electrode-to-electrode indicating that the reproducibility of the coatings is not sufficient. The Nafion-loading needs to be carefully controlled to produce a reproducible surface. The variation in the weight of Nafion on the surface had an RSD of 13% (0.0015 ± 0.0002 g), and is likely the source of variation. A couple of factors that may need to be better controlled are the homogeneity of the Nafion solution used for coating, and the volume applied to the electrode surface.

Table 6.2. Comparison of three electrodes with Nafion coating. Each electrode was used to analyze blood with 445 ppb Pb^{2+}. Two trials were performed on each film with a short cleaning step in 0.3 M HCl between. The exposure time was 15 minutes after which a deposition time of 180 s was used prior to ASV analysis.

Electrode	Peak Current (μA)	Peak Charge (μC)
1	0.218	0.505
	0.161	0.369
2	0.244	0.693
	0.177	0.419
3	0.248	0.478
	0.310	0.673
Average	**0.23 ± 0.05**	**0.5 ± 0.1**
Relative Standard Deviation	**24%**	**25%**

Another important point with Nafion-coated electrodes is how well the cationic analyte can be removed from the polymer. In order to obtain a clean background (i.e., no Pb signal) in 0.3 M HCl following Pb^{2+} exposure a series of cleaning steps were necessary. The cell was rinsed with 0.3 M HCl three times then filled with clean HCl, and 0.6 V was applied to the electrode for 3 min to oxidize any remaining Pb on the electrode. The cell was then rinsed again and a stripping voltammetric *i-E* curve was recorded, if a Pb signal was observed this procedure was repeated. When the electrode had been exposed to Pb^{2+} for a short amount of time (< 30 min) a clean background could be obtained after repeating the process 2-4 times. However, when the electrode was soaked in bovine blood containing Pb^{2+} for more than 12 h a clean background was not obtained even after repeating the cleaning procedure 10 times. Therefore, as long as the Nafion film is not in contact with the Pb^{2+} for extended periods of time a clean background can be obtained.

Another parameter investigated was the electrode sensitivity for Pb^{2+}. To study this, the blood was spiked with increasing concentrations of Pb^{2+} and a stripping voltammetric *i-E* curve was recorded for each concentration after 30 minutes of exposure to the Nafion film (Figure 6.4). With increasing Pb^{2+} concentration in solution, the stripping peak current increased at -0.55 V. A second oxidation peak, due to the Cl^-, was present in the voltammograms at a slightly more positive potential. The blood samples were run one after another using the same electrode with a cleaning step between runs. The increase in peak height is nearly linear (r = 0.98) with a sensitivity of 1.6 nA/ppb.

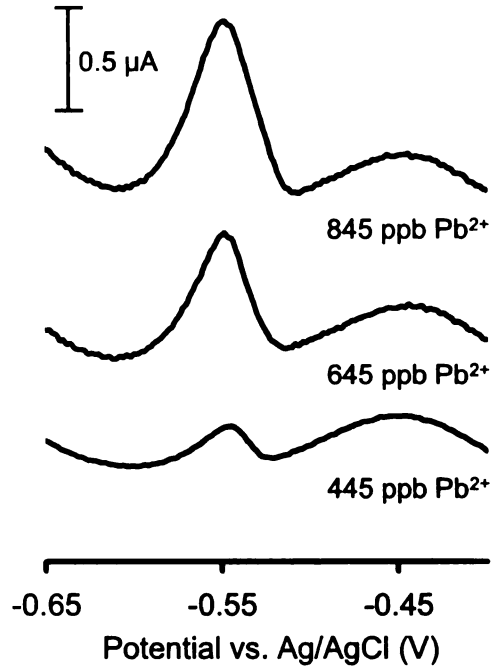

Figure 6.4. Stripping voltammetric *i-E* curves of Pb^{2+} in blood at varying concentrations. The bovine blood was mixed 1:5 with 0.3 M HCl. The electrode exposure time was 30 min. The deposition time was 180 s followed by ASV analysis. Curves are offset for clarity.

The cell setup in these experiments has the BDD electrodes mounted from the bottom with a Viton o-ring that is used to define the area exposed. When the electrode was removed from the cell, some of the Nafion film was also removed because it remained attached to the o-ring. This makes re-use of these electrodes impossible because of polymer film damage, making it necessary to fully remove Nafion for re-coating.

The solvent used for the colloidal Nafion was ethanol so this was the first choice for Nafion removal from the electrode surface. The electrode was wetted with ethanol then wiped with a disposable laboratory wipe to remove the bulk of the Nafion from the surface. Next, the electrode was sonicated in ethanol for 15

min. Because the diamond surface is rough and consists of many grains and grain boundaries it is possible that the Nafion may remain in these grain boundaries. To examine if there was any material in the grain boundaries atomic force microscopy (AFM) was used. Displayed in Figure 6.5 are three contour plot images of the BDD surface using different methods for Nafion removal: acetone (A), ethanol (B), acid washing and rehydrogenation (C). Comparing the images, the most defined grain structure is seen on the rehydrogenated surface (C). While the surface cleaned with ethanol (B) shows more definition in the grain boundaries than the acetone cleaned substrate (A), but is still not as clean as the rehydrogenated surface. The Nafion is not very soluble in the acetone, therefore, this was the least effective method, the bulk of the Nafion was removed from the surface by physical wiping, however, a significant amount remains in the grain boundaries. It seems the best way to fully remove any Nafion from the diamond surface is to use ethanol to remove most of the Nafion first followed by a standard acid washing and rehydrogenation procedure.

In summary, it appears that Nafion prevents fouling of the BDD electrode surface by components in blood. Using a 30 min exposure time the response was close to linear with a sensitivity of 1.6 nA/ppb. However, a more reproducible coating procedure needs to be adopted before this will be useful analytically. The disadvantage of an ionomer coating is that the response depends on the amount of time the electrode is in a solution prior to ASV.

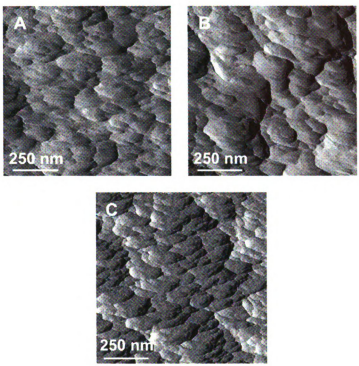

Figure 6.5. AFM contour plots of three BDD electrodes, taken in contact mode. The electrodes were coated in Nafion, which was removed with acetone (A), ethanol (B), and acid washing followed by rehydrogenation (C).

6.3.2. Sodium Dodecyl Sulfate

An alternative to protecting the surface with Nafion was to reduce the affinity of the proteins for the electrode surface. Hoyer and Jensen suggested that sodium dodecyl sulfate (SDS) could be used for this purpose to suppress electrode fouling.[35-37] They found that the SDS forms soluble aggregates with proteins in solution, and prevents their interaction with the surface. This was successfully applied to the ASV determination of Cd^{2+}, Pb^{2+}, and Cu^{2+} in fruit juice, beer, milk powder, and waste water using a rotating glassy carbon electrode.[36] They also found that SDS had little or no effect on the ASV signal for the metal ions at this electrode.[35, 36]

Hoyer used a concentration of SDS that was approximately 3 mM (1000 ppm) which is above the critical micelle concentration (CMC) for a high ionic strength solution.[37-39] The CMC of SDS in a pure aqueous solution is around 8 mM.[40] However, the CMC is strongly influenced by the ionic strength because the repulsion between head groups is the limiting factor in micelle formation, when the ionic strength is higher there is less repulsion, therefore, the micelle size is increased, and the CMC is decreased.[39] The effect of SDS on ASV measurements depends on many experimental parameters, including electrolyte and working electrode material, so it was necessary to determine the effect of the SDS using a BDD electrode in an HCl solution.[35]

To determine the effectiveness of SDS at protecting the diamond electrode surface in blood a 3 mM SDS in 0.3 M HCl solution was mixed with a Pb^{2+} sample. Rather than blood, 50 ppm bovine serum albumin (BSA) was added to a solution of 450 ppb Pb^{2+}, to simulate the blood matrix. The electrode response was first tested using a solution of Pb^{2+} in HCl. Next the Pb^{2+} solution containing BSA was tested in the HCl with SDS. Finally the electrode response was re-tested in Pb^{2+} in HCl. The electrode responses are presented in Figure 6.6. There was no significant difference in the Pb stripping response before or after the exposure to BSA, and the response is not suppressed in the presence of BSA. This indicates that BDD is not fouled by the BSA when introduced in a solution also containing SDS.

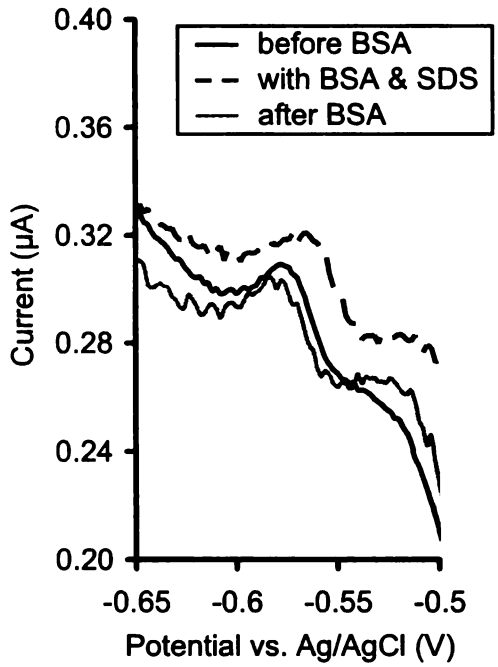

Figure 6.6. Stripping voltammetric *i-E* curves of 450 ppb Pb^{2+} solution mixed 1:5 with 0.3 M HCl. The solutions used before and after BSA exposure (black and grey solid lines) only contain Pb^{2+} and HCl. The other sample (dashed line) also contained 50 mg/L BSA and 3 mM SDS. The deposition time was 180 s.

In contrast to the initial measurements in blood (Figure 6.2), the addition of the SDS appears to prevent the proteins from fouling the bare BDD surface. This is important to allow measurement of Pb^{2+} on an uncoated surface with the addition of SDS to the blood prior to exposure to the BDD surface. However, the concentration of BSA in the test was only 50 mg/L, and in the blood the protein concentration is likely to be in the range of g/L. Therefore, it may be necessary to use much higher SDS concentrations for use in blood because of the higher concentration of protein.

6.4. Conclusions

While BDD cannot be used for blood analysis directly, there are a number of options available to prevent fouling of the surface, making it useful for this

measurement. A Nafion-coated electrode was able to be used for Pb^{2+} analysis, and had an approximately linear response with solution concentration. The advantage and disadvantage of the Nafion-coated electrodes is the preconcentration of Pb^{2+} in the polymer. While this can yield higher signals and sensitivity it also makes the measurement sensitive to the electrode exposure time. An alternative option to a coated electrode is a solution based aggregation of the proteins using an anionic surfactant such as SDS. Employing SDS in this sampling method is promising because even in the presence of albumin a very similar response was obtained for Pb^{2+} with the addition of SDS. The SDS prevented the protein from fouling the bare BDD.

6.5. References

(1) Goyer, R. A. In *Casarett & Doull's Toxicology: The Basic Science of Poisons,* 5th ed.; Klaassen, C. D., Ed.; McGraw-Hill: New York, 1996, pp 691-736.

(2) General Lead Information: Questions and Answers. http://www.cdc.gov/nceh/lead/faq/about.htm (accessed 2007)

(3) Plotkin, E.; McAleer, J. F.; Cordeiro, M. L.; Ackland, M. R.; Sheehan, T. M.; Braithwaite, R. A. *Clin. Chem.* **1997**, *43*, 2187-2189.

(4) Matson, W. R. Apparatus for stripping voltammetry. U.S. Patent 4,201,646, May 6, 1980

(5) Matson, W. R. Sampling system and analysis cell for stripping voltammetry. U.S. Patent 5,284,567, February 8, 1994

(6) Matson, W. R. Sampling system and analysis cell for stripping voltammetry. U.S. Patent 5,290,420, March 1, 1994

(7) Hoyer, B.; Florence, T. M.; Batley, G. E. *Anal. Chem.* **1987**, *59*, 1608-1614.

(8) Ibanez, J. C. V.; Lorente, M. M. F.; Suarez, J. R. C. *Quim. Anal. (Barcelona)* **1998**, *17*, 95-103.

(9) Jaenicke, S.; Sabarathinam, R. M.; Fleet, B.; Gunasingham, H. *Talanta* **1998**, *45*, 703-711.

(10) Banks, C. E.; Compton, R. G. *Analyst* **2004**, *129*, 678-683.

(11) Kruusma, J.; Banks, C. E.; Compton, R. G. *Anal. Bioanal. Chem.* **2004**, *379*, 700-706.

(12) Feldman, B.; D'Alessandro, A.; Osterloh, J. D.; Hata, B. H. *Clin. Chem.* **1995**, *41*, 557-563.

(13) Xu, J.; Granger, M. C.; Chen, Q.; Strojek, J. W.; Lister, T. E.; Swain, G. M. *Anal. Chem.* **1997**, *59*, 591A-597A.

(14) Xu, J.; Chen, Q.; Swain, G. M. *Anal. Chem.* **1998**, *70*, 3146-3154.

(15) Granger, M. C.; Witek, M.; Xu, J.; Wang, J.; Hupert, M.; Hanks, A.; Koppang, M. D.; Butler, J. E.; Lucazeau, G.; Mermoux, M.; Strojek, J. W.; Swain, G. M. *Anal. Chem.* **2000**, *72*, 3793-3804.

(16) Hupert, M.; Muck, A.; Wang, J.; Stotter, J.; Cvackova, Z.; Haymond, S.; Show, Y.; Swain, G. M. *Diamond Relat. Mater.* **2003**, *12*, 1940-1949.

(17) Shin, D.; Tryk, D. A.; Fujishima, A.; Merkoci, A.; Wang, J. *Electroanal.* **2005**, *17*, 305-311.

(18) Smart, R. B.; Stewart, E. E. *Environ. Sci. Technol.* **1985**, *19*, 137-140.

(19) Kamei, K.-i.; Mie, M.; Yanagida, Y.; Aizawa, M.; Kobatake, E. *Sens. Actuators, B* **2004**, *99*, 106-112.

(20) Wang, J.; Hutchins, L. D. *Anal. Chem.* **1985**, *57*, 1536-1541.

(21) Wang, J.; Hutchins-Kumar, L. D. *Anal. Chem.* **1986**, *58*, 402-407.

(22) Kuhn, L. S.; Weber, S. G.; Ismail, K. Z. *Anal. Chem.* **1989**, *61*, 303-309.

(23) Hoyer, B.; Jensen, N. *Talanta* **1995**, *42*, 767-773.

(24) Marinesco, S.; Carew, T. J. *J. Neurosci. Methods* **2002**, *117*, 87-97.

(25) Kristensen, E. W.; Kuhr, W. G.; Wightman, R. M. *Anal. Chem.* **1987**, *59*, 1752-1757.

(26) Ibanex, J. C. V.; Lorente, M. M. F.; Suarez, J. R. C. *Quimica Analytica* **1998**, *17*, 95-103.

(27) Liu, K.-z.; Wu, Q.-g.; Liu, H.-l. *Analyst* **1990**, *115*, 835-837.

(28) Dalangin, R. R.; Gunasingham, H. *Anal. Chim. Acta* **1994**, *291*, 81-87.

(29) Dam, M. E. R.; Thomsen, K. N.; Pickup, P. G.; Schroder, K. H. *Electroanal.* **1995**, *7*, 70-78.

(30) Matysik, F.-M.; Matysik, S.; Vrett, A. M. O.; Brett, C. M. A. *Anal. Chem.* **1997**, *69*, 1651-1656.

(31) Hurst, M. P.; Bruland, K. W. *Anal. Chim. Acta* **2005**, *546*, 68-78.

(32) Kefala, G.; Economou, A. *Anal. Chim. Acta* **2006**, *576*, 283-289.

(33) Legeai, S. *Anal. Chim. Acta* **2006**, *560*, 184-190.

(34) Zook, L. A.; Leddy, J. *Anal. Chem.* **1996**, *68*, 3793-3796.

(35) Hoyer, B.; Jensen, N. *Electrochem. Commun.* **2003**, *5*, 257-261.

(36) Hoyer, B.; Jensen, N. *Analyst* **2004**, *128*, 751-754.

(37) Hoyer, B.; Jensen, N. *Electroanal.* **2005**, *17*, 2037-2042.

(38) Emerson, M.; Holtzer, A. *J. Phys. Chem.* **1967**, *71*, 1898-1907.

(39) Helenius, A.; McCaslin, D. R.; Fries, E.; Tanford, C. *Methods Enzymol.* **1979**, *56*, 734.

(40) Bales, B. L.; Messina, L.; Vidal, A.; Peric, M.; Nascimento, O. R. *Journal of Physical Chemistry B* **2998**, *102*, 10347-10358.

CHAPTER 7

CONCLUSIONS

The overall aim of this work was to fully evaluate and understand the properties of boron-doped diamond (BDD) as they related to its use in anodic stripping voltammetric (ASV) measurements. Initial studies in this area showed that BDD was a suitable electrode with ASV for metal ion analysis in river water, tap water, soil, and sludge. In order to more fully evaluate BDD as an alternative electrode to Hg for ASV several studies were conducted: (i) comparison of the electrochemical properties and response with the traditional Hg electrode, (ii) exploration of the utility of the material in microgravity applications, (iii) determination of the usefulness of BDD for more complex matrices (e.g., urine, blood), and (iv) investigation of ways of preventing electrode fouling (e.g., coatings, complexing agents) in solutions containing high protein concentrations (e.g., whole blood).

In addition to having many of the desirable features of Hg, BDD has some inherent advantages; it is non-volatile and non-toxic. This makes it an advantageous electrode choice for clinical and environmental analysis. The response of BDD was compared to a Hg-coated glassy carbon (Hg-GC) electrode in terms of the analytical figures of merit, nature of metal deposition, and stripping voltammetric peak potentials and shapes. BDD has a wider anodic potential limit and a lower background current density than Hg. Overall, the detection figures of merit for BDD are as good or superior to those for Hg-GC. Both BDD and Hg-GC provided detection limits for all the metal ions (Zn^{2+}, Cd^{2+},

Pb^{2+}, Cu^{2+}, and Ag^{+}) in the mid to low ppb range (S/N ≥ 3). The biggest difference between the two electrodes was the magnitude of the stripping peak current and charge, which are greater for Hg-GC. This is because of the large volume of Hg into which the foreign metal can deposit compared to the surface area of BDD available for deposition. The greater amount of metal deposited on Hg-GC resulted in a higher sensitivity, but this was offset by a comparable reduction in the background noise for BDD, which resulted in comparable or lower limit of detection values. Electrochemical measurements revealed that reduced sensitivity due to incomplete metal oxidation or metal phase detachment was not an issue for these BDD films.

A significant effort was spent developing BDD for use in water supply monitoring on-board the International Space Station (ISS). The properties of BDD (e.g., non-toxic, non-volatile) made it attractive for this application. The previously developed ground-based ASV method was modified for microgravity use. A concentrated buffer solution was developed to adjust the solution conditions (e.g., pH, electrolyte concentration), and a prototype cell for microgravity was developed. The prototype cell was a fully sealed electrochemical cell that allowed introduction of sample through luer fittings compatible with the current NASA water sampling system. The method provided accurate concentration determinations for Ag^{+}, Cu^{2+}, Pb^{2+}, and Cd^{2+}, and the response was unaffected by the increased pH (5.2), or the minerals added for taste (Ca^{2+} and Mg^{2+} salts). Elimination of the N_2 purge step to remove dissolved O_2 was not a problem for Ag^{+} and Cd^{2+} analysis; however, the presence of

dissolved O_2 did affect the Pb^{2+} and Cu^{2+} analysis. The use of an oxygen scavenging molecule (ascorbic acid) to chemically remove the O_2 mitigated this problem to a large extent. BDD exhibited good long-term response stability for Ag^+ (<10% relative standard deviation in response over 90 days). Analysis of simulated water samples in the microgravity cell using BDD yielded accurate Ag^+ concentrations (< 5% error).

Once BDD had been successfully applied to environmental and water samples, the next type investigated was biological samples (e.g., blood, urine) to probe the fouling resistance of the surface in more complex matrices. A urine simulant containing Cd^{2+} was used and a linear calibration curve was obtained over a range of 2 orders of magnitude (10–250 ppb), and the response was reproducible from electrode-to-electrode (RSD 6%). Urine contains compounds that can complex the Cd^{2+} (e.g., ammonia, lactic acid, citric acid), which reduced the activity of free Cd^{2+} thereby reducing the electrochemical response. To obtain the highest electrochemical signal and accurate concentration determination for Cd^{2+}, a digestion step or other purification step is necessary. While the simulant contains many of the major components of urine, it did not contain any protein, therefore, real urine (rat) was tested as well. BDD performed adequately, and an increased signal was observed for increasing concentrations of Cd^{2+}. The electrode showed no fouling effects over a 6-hour period.

One of the more complex biological matrices is blood, and for metal ion analysis, it is necessary to use the whole blood rather than just a plasma sample.

Blood contains a large amount of proteins that can passivate the electrode surface, and even though BDD is resistant to fouling, it cannot be used directly in whole blood. Two different fouling prevention strategies were investigated: a polymer coating (Nafion) and an added surfactant to aggregate with the proteins in solution (sodium dodecyl sulfate). BDD was successfully coated with Nafion, and was able to be used for Pb^{2+} analysis with a linear calibration response (r^2>0.98). However, Nafion coating does have some disadvantages. First, the reproducibility of the coating can affect the reproducibility of the measurement from run-to-run. Second, the analysis is time dependent because Nafion is a cation-exchange polymer, and the longer it remains in contact with the Pb^{2+} solution the more preconcentration occurs increasing the electrochemical signal. The solution-based aggregation of protein with sodium dodecyl sulfate (SDS) is a promising option, and even in the presence of albumin the BDD showed very similar electrochemical response to the analysis in standard solutions. The benefit of the solution based method is that it is much easier to add a reproducible amount of SDS to a solution than to have a reproducible polymer coating.

Overall, BDD performed well for ASV analysis, and is definitely a suitable alternate to Hg. The inert nature of the electrode material and the ability to reuse the surface for multiple replicate analyses are definite advantages. In this work, the utility of BDD was demonstrated for many different sample types; however, one thing that was not specifically addressed was potential interferences from intermetallic compound formation.

Intermetallics can form during the deposition from a sample that contains different metal ions. This tends to be more of a problem on a solid electrode, such as BDD. In a Hg electrode the metal will form an amalgam, which helps to reduce formation of intermetallic species by physically separating the metals. On a solid electrode such as BDD the different metals can co-deposit at the surface and form an intermetallic. The intermetallic formation can affect ASV analysis by shifting the potential at which a metal is detected because the E^0 value for a pure metal will be different from an intermetallic.

In the previous studies using BDD to detect multiple metal ions in a standard reference material there was some evidence for the formation of intermetallics on BDD; a secondary peak associated with the Cu peak was observed. However, the concentrations of the metals in the standard reference material were still able to be accurately determined. While the formation of intermetallics did not pose a problem in the concentration determination in this particular sample it is worth investigating further to determine the utility of BDD in multimetal solutions.